Spring 1-1-2012

# Model Development and Experimental Validation of Pressure Independent Hydronic Circuits

Justin Thomas Bellucci
*University of Colorado at Boulder*, justin.bellucci@colorado.edu

# MODEL DEVELOPMENT AND EXPERIMENTAL VALIDATION OF PRESURE INDEPENDENT HYDRONIC CIRCUITS

by

JUSTIN BELLUCCI

B.S. University of Colorado, Boulder

2008

A thesis submitted to the

Faculty of the Graduate School of the

University of Colorado in partial fulfillment

of the requirement for the degree of

Civil Engineering

2012

This thesis entitled:
Model Development and Experimental Validation of
Pressure Independent Hydronic Circuits
written by Justin Bellucci
has been approved for the Department of Civil Engineering

_____

Prof. Gregor Henze, Ph.D., P.E.

_____

Marc Thuillard, Ph.D.

Date May 11, 2012

The final copy of this thesis has been examined by the signatories, and we
find that both the content and the form meet acceptable presentation standards of
scholarly work in the above mentioned discipline.

# Abstract

Bellucci, Justin (M.S., Civil Engineering)

Model Development and Experimental Validation of Pressure Independent Hydronic Circuits

Thesis directed by Professor Gregor Henze

Computer modeling is quickly becoming a more accessible method to evaluate the performance of complex building systems, due in part to the recent advance in computing power over the last decade. Rising energy costs, stricter building codes, the threat of global climate change and governmental pressure have all influenced building owners, architects, engineers and system operators to design and operate the world's building stock in a more energy efficient manner. Particularly important in large buildings and campuses are the hydronic flow networks that deliver chilled water to the cooling coils in air handling units for the purpose of regulating temperature and humidity in occupied spaces. Large buildings are especially dominated by cooling loads, thus making it a priority for many to evaluate such hydronic systems for their energy performance characteristics. The design and operation of these hydronic systems are being optimized with the help of computers, in both new building stock and retrofits in order to reduce energy consumption.

A common problem that has been well documented over the last few decades is that of delta-T degradation, the decrease in the temperature difference between the supply and return flow of water from the design value over time. Most central plants are designed to deliver chilled water to respective buildings or air handling units at a relatively constant temperature. Typically chilled water is delivered to each branch circuit, which for this example will consist of piping, a cooling coil and a control valve. Coils are selected based on the cooling power needed and a design delta-T value. The flow rate of water through each cooling coil is adjusted to meet demand; therefore with a constant delta-T, an increase in cooling demand would necessitate a proportional increase in the flow rate of water.

There is a slight disconnect between manufacturer data on cooling coils and what actually happens in real systems. Coils are selected based on design values and assumed supply conditions, although installed characteristics of the coil can be quite different from that of the manufacturer specification sheet. For instance, a coil may be selected based on a specific supply water temperature, but if the supply water temperature rises, due to an overloaded central plant, the amount of cooling power delivered will be considerably less then design value. Coil performance can also degrade over time due to coil fouling on either the waterside or airside. Many causes of these parameter fluctuations are well known, however the consequences of such fluctuations are not fully documented. In order to better design and optimize intelligent control devices, a better understanding of the performance of cooling coils is needed. This documentation attempts to combine experimental data with computer simulation to provide a visual guide to how fluctuations in supply water flow rate, supply water temperature, supply air temperature, supply air flow rate and supply air humidity affect cooling power achieved from various cooling coils in operation. Experimental data is used in conjunction with computer simulation to investigate how performances of these coils are affected.

I want to thank my parents for their unparalleled support over the years. I could not have done this without you both. I also want to thank my thesis advisor Gregor Henze and Marc Thuillard for their dedication and devotion to my research.

# Contents

# 1 Introduction and Motivation

Computer modeling is quickly becoming a more accessible method to evaluate the performance of complex building systems, due in part to the recent advance in computing power over the last decade. Rising energy costs, stricter building codes, the threat of global climate change and governmental pressure have all influenced building owners, architects, engineers and system operators to design and operate the world's building stock in a more energy efficient manner. Particularly important in large buildings and campuses are the hydronic flow networks that deliver chilled water to the cooling coils in air handling units for the purpose of regulating temperature and humidity in occupied spaces. Large buildings are especially dominated by cooling loads, thus making it a priority for many to evaluate such hydronic systems for their energy performance characteristics. The design and operation of these hydronic systems are being optimized with the help of computers, in both new building stock and retrofits in order to reduce energy consumption.

A common problem that has been well documented over the last few decades is that of delta-T degradation, the decrease in the temperature difference between the supply and return flow of water from the design value over time. Most central plants are designed to deliver chilled water to respective buildings or air handling units at a relatively constant temperature. Typically chilled water is delivered to each branch circuit, which for this example will consist of piping, a cooling coil and a control valve. Coils are selected based on the cooling power needed and a design delta-T value. The flow rate of water through each cooling coil is adjusted to meet demand; therefore with a constant delta-T, an increase in cooling demand would necessitate a proportional increase in the flow rate of water as seen in Equation 1.

$$\dot{Q} = \dot{m}_L C_P \Delta T \tag{1}$$

Unfortunately this ideal case does not always happen in many systems. If delta-T begins to degrade, load and flow will not be in sync. For example, if a particular cooling power is desired and delta-T is less then design-value, the flow rate will have to be increased to compensate for the increased load and the decease in delta-T. If a coil is accurately selected for a particular system there will be a maximum amount of power that that coil can deliver for any given water flow rate. If the load increases and delta-T decreases, the coil will have to operate out of its optimal range. This will result in coil saturation, the point at which a significant increase in water flow rate does not lead to any

significant increase in cooling power. As delta-T degrades the return water temperature will also be lower, therefore leading to decreased chiller efficiency. A theoretical approximation for the increase in pumping power can be extracted from one of the pump affinity laws. It simply states that pump motor speed is proportional to the cube of the flow rate of water; therefore an increase in flow rate will require considerable more power from the pump. This is of great concern in large buildings and campus systems as there is great potential to save considerable distribution energy over the life of such systems.

There are many well-documented reasons for delta-T degradation, some of which can be avoided and some of which cannot. In many cases improper sizing of coils lead to increased flow rates under part load conditions. For example, in multi-building campus systems, coils are often selected for a delta-T that is lower then the central plant delta-T. This can happen because multiple engineers often design various systems. In many cases engineers will also attempt to minimize the waterside pressure drop by selecting a dual-row coil rather then a full-row coil. Dual-row coils have a lower tube velocity and therefore a lower waterside pressure drop. Full-row coils have a higher water velocity, which improves heat transfer rates at part-load conditions (Taylor 2002). Other common causes are improper control valve sizing, use of three-way control valves, loop configuration, improper control strategies, and using the wrong setpoints. Many of these causes have been documented over the years and will be covered in greater detail in the next section of this paper, however it is important to understand some of the basic causes of delta-T degradation to appreciate past and current efforts being made to mitigate the problem.

Among past efforts to reduce delta-T degradation is eliminating the use of three-way control valves in system design. A shift in using two-way characterized control valves (CCVs) and a balancing valve for each coil can help in part load conditions. However, if the circuit were not properly balanced, the problem of low delta-T would persist or even possibly get worse. Many established companies in the building automation and control industry began designing pressure independent valves (PIVs). These new valves essentially maintain a constant pressure across the valve and therefore eliminate the need for a separate balancing valve in the circuit. Most modern buildings are now controlled by a building management system (BMS), which is programmed to monitor and maintain indoor environment and the systems that control the building. In recent years there has been a convergence of building technology and information technology. Buildings and building components are being equipped with more intelligence, thus leading to the acquisition of more data on building systems which allow for better control and ultimately increased energy

savings. A well-established Swiss company is currently designing more intelligent control valves, which not only regulate water flow but also measure and record water temperature and flow rate. These new valves receive a signal from the DDC system, and then use its flow and temperature readings to help increase delta-T and optimize the energy saving potential at the cooling coil level. In order to develop more robust control strategies for such intelligent devices, it is important to understand how the characteristics of cooling coils are affected by changing input parameters such as supply water temperature, mixed air temperature, mixed air humidity, and airflow rate.

There is a slight disconnect between manufacturer data on cooling coils and what actually happens in real systems. Coils are selected based on design values and assumed supply conditions, but as stated previously the installed characteristics of the coil can be quite different from that of the manufacturer specification sheet. For instance, a coil may be selected based on a specific supply water temperature, but if the supply water temperature rises, due to an overloaded central plant, the amount of cooling power delivered will be considerably less then design value. Similar trends are observed for changing mixed air temperature, mixed air humidity and airflow rate. Coil performance can also degrade over time due to coil fouling on either the waterside or airside. Many causes of these parameter fluctuations are well known, however the consequences of such fluctuations are not fully documented. All of these factors combined make it a difficult task to develop control strategies for intelligent devices, which in turn control cooling coils under such variable conditions.

Most of the current documentation on cooling coil performance is for selection purposes only and is based on experimental data from coil manufacturers. Also presented by much of the industry, is the typical cooling coil curve that plots power vs. flow rate of water. By using a combination of computer simulation and actual field data acquired at the University of Colorado Boulder and the Massachusetts Institute of Technology (MIT), this research will provide a visual documentation on how cooling coil heat transfer rates change with varying input parameters. This documentation will also serve as a guide to recommend strategies for the purpose of intelligently limiting the waterside delta-T and to limit the operation of coils in the saturated zone.

# 2 Literature Review

## 2.1 – Delta-T Degradation

Large buildings are primarily cooling dominated due to the high internal gains that occur and therefore require chilled water distribution during the majority of operating hours. Typically chilled water is pumped to each building and distributed to each respective cooling coil in order to meet the demand in a particular zone. Most large buildings and campuses house a central plant, which is responsible for delivering water through the complex maze of pipes, pumps, valves and coils. Many of these central plants are designed for a relatively constant design delta-T, but in most cases delta-T falls well below design values. With a constant delta-T, load (Watts) and flow (l/s) are proportional. An increase in water mass flow will result in an increase in cooling power, but when delta-T degrades load and flow will not be in sync. When the waterside temperature difference decreases water mass flow will need to increase to compensate and maintain the cooling power desired as illustrated in Equation 1. The return water temperature will also be lower and therefore will reduce chiller efficiency. The combination of increased pumping power and reduction in chiller efficiency contribute to a considerable amount of wasted energy in many hydronic systems. The following body of research reviews three distinct approaches to mitigating delta-T degradation as well as case studies in which many of the methods described are implemented.

Much of the existing literature written about delta-T degradation attempts to address the problem by offering a series of qualitative recommendations, which are mostly based on experience from industry experts. Many of these recommendations are aimed at keeping the waterside temperature difference high in the hopes that at part load conditions delta-T will then be above design levels. Let us examine an example that Fiorino (1999) uses to illustrate the case for achieving a high delta-T, which he recommends to be a value at or above 8.5 ˚C. Imagine a crossflow cooling coil with a 5.6 ˚C supply water temperature, a 26.7 ˚C mixed air temperature and an 11.7 ˚C supply air temperature. This is a typical configuration with nonlinear characteristics in which 80% of cooling output can be achieved with only 50% of the design chilled water flow rate. For this example Fiorino (1999), points out that 100% power is achieved at 100% design water flow with a delta-T of 8.5 ˚C. At part load conditions he recommends a 60% increase in the design delta-T value to achieve 80% of the design cooling load. The opposite effect is seen when an increase of 100% of the water flow over design will only yield a 15% increase in cooling power with a delta-T that is 40% less then design value. This example illustrates the simple point that cooling power is very sensitive to delta-T

setpoints, with the assumption that the supply water temperature, mixed air temperature and supply air temperature are constant.

The approach that Fiorino (1999) takes towards achieving a high delta-T is to focus on the terminal devices such as cooling coils and control valves while offering specific control strategies to raise delta-T. He argues that the symptoms of delta-T syndrome are often misinterpreted as poor cooling performance, which can be attributed to a lack of chilling capacity. Shifting the focus from a capital intensive measure of upgrading the central plant to the individual branches of the circuit is recommended. Twenty-five best practice recommendations were presented after being implemented in a Dallas factory. Fiorino (1999) recommends the use of two-way equal percentage control valves, robust actuators with digital control, recycling of chilled water for use in coils that only need to meet sensible loads, and accurate attention to setpoints and PI parameters within control strategies. All of the recommendations for the Dallas facility were successful at raising delta-T values by 50% from 6.7 ˚C to 10 ˚C.

Conventionally, the design of large chilled water distribution systems used a primary/secondary approach to the central plant design. These systems included constant speed pumps and chillers that consumed large amounts of energy due to the constant pumping power required to maintain flow to the furthest coil. Typical design included a bypass line, which separated the secondary side from the primary side, and in most cases three-way control valves were used in conjunction with a balancing valve at the coil level (Taylor 2002). This configuration prevented the pumps from operating against a closed control valve, which can be detrimental to the system. This configuration posed a few problems though, especially under part load conditions. Two basic approaches at controlling such systems are typically used; flow based control and load based control, each of which has its faults when delta-T falls below design levels. In the flow based control strategy the approach is to keep the primary flow larger then the secondary flow. Flow is typically measured in the common leg and when the flow is sensed to be at a minimum threshold another chiller is brought online. This strategy works fine when everything is in sync but when delta-T falls below design levels chillers will not operate at peak efficiency. This also wastes considerable pump energy.

The load-based strategy starts and stops chillers based on the load on the system, which can be indicated by the return water temperature. Another chiller will not be brought online until the current chiller is operating at peak load. If delta-T degrades below design level, the return water temperature will rise sending a signal to the control valves to demand more flow. The valves will open, water flow will increase and a portion of the flow will inevitably be diverted through the

bypass valve, thus raising the return water temperature even higher. In this control strategy the chillers would be unaware of any changes and be kept offline. Considerable energy would be wasted and comfort would be difficult to achieve. Taylor (2002) offers suggestions on how to maximize delta-T as well as ways to design systems to accommodate for low delta-Ts that he says will inevitably occur. He claims that the most common cause of low delta-T is improper setpoints of the supply air temperature. A drop in supply air temperature from 54 °F to 51 °F can cause the mass flow of water to double and cause delta-T to drop in half (Taylor 2002).

Another common error is in the selection of system components such as the coil and the control valve. It is very common that multiple engineers work on projects over the years on large campus hydronic projects. This can cause problems if there is not a strict set of guidelines to follow. Some engineers may oversize coils or choose a coil with a lower delta-T then the plant may be designed for. If an engineer chooses a coil to maximize delta-T this may have a negative influence on the airside pressure drop. More rows of tubing and more fins in the coil will increase airside resistance and therefore may require a larger fan to overcome the large pressure drop. Just the opposite can happen when a coil is selected to minimize the airside pressure drop, neglecting the high delta-T required. Taylor points out that a careful balance between airside and waterside pressure drops is very important.

Variable speed drives are recently being implemented in many systems to reduce pumping power needed. Because VFDs greatly reduce the amount of energy that pumps consume, it is common to have primary pumps and chillers in the central plant and secondary pumps located at the building entrance. Two-way valves and VFD driven pumps can be used for each building and therefore will eliminate the need for the primary pumps to operate at constant speed regardless of the load on the system. Replacing three-way valves with electronic pressure independent control valves (ePIVs) reduces the need for separate balancing valves. Pressure independent valves essentially balance themselves, and in conjunction with efficient VFD pumps considerable increases in delta-T can be realized. Taylor points out that care should be taken when choosing control valves as not to oversize them. An oversized valve will have trouble controlling at low flow and will inevitably begin to hunt. Hunting is a term used to describe the oscillation that can be seen when a control valve tries to maintain setpoint but unfortunately cannot. This can cause considerable wear and tear on the actuator, thus reducing its operating life.

Up to this point the existing literature has offered a qualitative analysis to the delta-T syndrome problem found in many hydronic systems and has offered suggestions on how to raise delta-T based

on expert knowledge. Henze and Floss (2011) offer a different approach towards solving the issue of low delta-T, although their approach and recommendations are applied to district heating systems. They argue that there are many similarities between cooling and heating applications most notably an increase in water flow rate when delta-T degrades. Multiple faults in system design were identified based on previous research and personal experience. Among the faults identified were hydraulic network imbalance, control valve sizing, incorrect valve characteristics and incorrect control loop parameters. A dynamic simulation was conducted to illustrate the contribution that each of these faults has on delta-T degradation. Henze and Floss (2011) identified control valve sizing and inherent valve characteristics and network balancing as the most important of the identified parameters. When compared with a properly tuned system, delta-T degradation of 5-6 K was predicted in the heating application. Henze and Floss (2011) also point out, based on research from Wirths, that a degradation of 6 K in a district heating application would see an increase in primary energy consumption from 4 to 12%. The considerable savings recognized by these system improvements are realized in many retrofit projects.

The University of California Riverside campus was experiencing many problems with their chilled water system, which resulted in low a low waterside temperature difference and even negative differential pressure measurements. The system experienced negative delta-P measurements at points furthest from the central plant and high delta-P measurements in buildings close to the central plant. The low delta-P that occurred furthest from the central plant resulted in complaints about comfort because the cooling coils were being starved and therefore could not meet demand. The high delta-P that occurred near the central plant forced control valves open, which consequently lowered delta-T. The lower waterside temperature difference resulted in loss of thermal energy storage capacity since the capacity of the TES system is directly proportional to the difference between the supply and return chilled water temperatures. The result of such degradation contributed to increased pumping power and reduced comfort. Many of the older buildings on the campus were designed using constant speed pumps in a primary/secondary/tertiary configuration. The existing control strategy forced pumps to work at full capacity to overcome low delta-Ps. This was never achieved resulting in a lower return water temperature and a lower then design delta-T. Hyman and Little (2004) points out that a 0.5˚C drop in delta-T results in a 5% loss in TES capacity. As the campus grew, the existing TES system could no longer offset the cooling demand.

A lack of chilled water system design standards during the rapid expansion of the university resulted in buildings designed with different interfaces and control strategies. In many cases three-

way control valves were modified to act like two-way control valves, by closing off the bypass line. This resulted in poor control at lower flows adding to the low delta-T problem. Many systems were also designed with low delta-T cooling coils in hopes to decrease the airside pressure drop. It was evident that a serious retrofit was necessary. In the ASHRAE paper by Hyman and Little (2004) it was recommended that UCR replace the existing pumps and valves with VFD driven pumps and PICVs respectively. PICVs provide the proper flow regardless of the differential pressure while the additional VFD driven pumps help overcome the low differential pressure problem. Following the retrofit the UCR campus had for the first time experienced positive delta-P at the furthest buildings and recorded an increase in delta-T, which inevitably lead to an increase in comfort levels. The differential pressure increased from negative 172 kPa to positive 34 kPa while the central plant now experiences an 11°C delta-T. As a result the VFDs for the most remote buildings now operate at minimum speed.

The University of California, San Diego experienced similar problems with their chilled water distribution system as with the previous case study. Low delta-T persisted at low loads. This is a significant problem when the central chillers are designed to operate at a particular delta-T. For the majority of the year the central plant did not operate at design conditions and therefore the chillers operated outside their optimal range. UC San Diego attributed the problem to the failure of cooling coils to optimize heat exchange during part load conditions. Most of the buildings on campus were equipped with characteristic control valves (CCVs), which are pressure-dependent. A drop in pressure across the valve can cause the valve to open further, resulting in excess flow and an even lower pressure drop. UCSD facilities management implemented two measures to raise delta-T, first of which was to optimize the existing control strategy on central plant pumps and second to replace 75 valves in 17 buildings with pressure independent control valves (PICVs) at a cost of $975,000. The Green Building Research Center, at the University of California, Berkeley (Dilliot 2008) conducted a post analysis on savings and reported an annual energy savings of 7,375,000 kWh or $650,000.

Eglin Air Force Base in Northwest Florida originally designed the central plant based on a primary/secondary configuration with tertiary pumps at remote buildings, but because of early budget constraints they could not install the necessary variable speed drives on the pumps. This resulted in a considerable amount of wasted pumping power with an average energy consumption of 4.16 million kWh. A significant retrofit was made in 2008 by installing sixty-two PICCVs in conjunction with VFDs on the secondary and tertiary pumps. The pressure independent valves are

able to absorb the excess pressure in the system that occurs in variable speed systems. With the addition of the variable speed pumps and PICCV's, Eglin was able to eliminate six building booster pumps. The secondary pumps that once operated at 100% capacity now operate at 50 to 60% of capacity, resulting in an annual energy savings of $669,500 (Arnold 2007).

Another advantage of using pressure independent valves is that they maintain a constant pressure difference across the valve, regardless of variations in flow, thus eliminating the need for separate balancing valves. Traditionally three-way valves were used in conjunction with a balancing valve to balance each individual coil. Coils that are further away from the central plant experience greater pressure drop then coils close to the central plant. In order to make sure that the most remote coils received adequate flow the pressure drop at each coil can be adjusted using a balancing valve. An improperly balanced system has been shown to contribute to the low delta-T found in many systems. Balancing can become a significant problem when constant speed systems are converted to variable flow systems. Shell Point Retirement Community in Fort Myers, Florida has one of the largest thermal energy storage systems in the United States. The diversity and layout of the property has challenged the facilities maintenance to solve the low delta-T problem that occurred due to numerous three-way control valves that were originally installed at various air-handling units. The central chillers and pumps were updated with variable-frequency drives thus increasing efficiency. This had a negative impact on older buildings in which three-way control valves were installed. According to the project-development engineer at Shell Point, balancing these structures would be costly, burdensome, and questionable in terms of accuracy (Arnold 2007). Approximately forty PICCVs were installed throughout the community eliminating the need for costly balancing and maintenance issues previously experienced with pressure dependent valves.

## 2.2 – Cooling Coil Models

Due to the complex nature of heat exchangers and the increase in the use of computer simulation, there have been quite a few models developed over the last thirty years that attempt to solve for the exiting thermodynamic states of both air and water. Much of the following literature focuses on the development of models for cooling coils, which are the primary piece of heat exchange equipment in most modern commercial hydronic cooling systems. The cooling coil is an important piece of equipment because it removes both moisture and sensible heat from the entering air. In the majority of cases, both sensible and latent heat transfer is coupled, thus producing a nonlinear curve on the psychrometric chart. The coupled heat and mass transfer makes it very

difficult to solve the complex differential heat transfer equations across the coil. Much of the existing literature on cooling coils can be categorized into four types of coil models, dynamic, lumped, decoupled and steady state. Dynamic models are often used in the development of feedback controllers in which a time variant solution is necessary. These types of models are often very computationally intensive and require an in-depth understanding of coil parameters such as coil size and material properties. Lumped models consider the coil as a single system and lump parameters such as thermal resistance, convective resistance and conduction. Decoupled models have been developed that attempt to separate sensible and latent heat transfer modes in which computational efficiency is increased. Finally, many steady state models have been developed that use simplified relationships for the governing differential equations that describe heat transfer rates across the coil. Many of these models use an effectiveness-NTU approach to simplify the complex heat transfer mechanism, although many times this is only applicable to the sensible portion of the coil model and does not cover mass transfer on the latent side.

Most recently Braun and Zhou (2007) developed a simplified dynamic model that solves for both sensible and latent heat transfer using a combination of effectiveness-NTU relationships integrated with energy balance differential equations. Their research focused on building the most comprehensive dynamic model that was computationally efficient to be used in most modeling programs. They used effectiveness-NTU relationships to describe the resistance on the airside for both sensible and latent portions of the model. They defined the airside resistance as the inverse of the airside effectiveness and capacitance. The airside effectiveness defined was coupled to include both fin efficiency and airside convection coefficients. Similar relationships were used on the latent side to include both heat and mass transfer. Their coil model proved to execute 1000 times faster then real-time on a 1.2 GHz personal computer proving to be very useful for long-term simulations.

A year later Zhou and Braun (2008) developed a forward and inverse model for transient coil performance. The forward model solves the differential equations describing energy transfer using physical parameters of the actual coil. Their inverse model employs an approach that separates the dry and wet portions of the coil combined with a lumped parameter solution for each row of the coil. They use an effectiveness-NTU relationship similar to their previous work when solving for the airside resistance as well as lumped parameter estimation for coil capacitance. Because initial boundary conditions are needed before conducting the simulation they use a quasi-static method to solve for the initial conditions. The lumped parameters were determined from regression analysis of

actual coils and implemented as a simplification to the inverse model. The models developed proved to be computationally efficient and are useful for time variant applications.

Wang et al. (2007) proposed a different approach to dynamic modeling of cooling coils by decoupling the sensible and latent heat transfer mechanisms. They used a finite element method, which treats each node of the coil as a crossflow heat exchanger. Since it is very difficult to solve for the coupled heat and mass transfer at each node they claim that for a small portion of the coil the sensible heat ratio remains constant. With this assumption they attempt to decouple the sensible and latent portions of the model using the effectiveness-NTU method. This simplification allows the sensible and latent differential equations to be solved more effectively although an iterative approach is needed to solve for the SHR and humidity ratio saturation curve slope.

Because of the complexity of transient dehumidifying coil models, many steady state models have been developed over the years. Lemort and Lebrun (2008) built a steady state model by simplifying a reference model in which both sensible and latent portions are described simultaneously, lumping coil geometry into the thermal resistance on the waterside. The classical effectiveness-NTU method is used to express the airside effectiveness, which is then used to solve for the total sensible heat transfer of the coil. A similar method is used to solve for the latent portion using a fictitious heat exchanger in which enthalpies are defined for both the airside and for the surface temperature of the entering and exiting waterside states. Excluding the waterside calculations, and solving for only the airside simplified this model further. The simplified model proved only to be sufficient at solving for total energy consumption over long periods of time due to the simplified nature of the calculations involved and the assumptions made.

Even further simplification of a coiling coil was conducted by Wetter (1998), in which a steady state dry coil model was built using the effectiveness-NTU relationship. This model was used for yearly energy calculations with time steps of ten minutes or more. The main purpose of this simplified model, in which the only geometrical information needed was cross sectional data, was to provide insight to energy consumption at part load conditions. The model described part load behavior at nominal conditions using a dimensionless variation of the heat transfer with change of mass flow and temperature on the water and airside. Only explicit equations were used to solve for both the water and airside, which greatly improved computational efficiency.

A slightly more complex steady state model was built by Brandemuehl et al. (1993), which took into account geometrical information of the coil and solved for dry, wet and partially wet coil states using the effectiveness-NTU method coupled with a ratio approximation for the partially wet

scenario as well as an enthalpy based method for the totally wet case. In order to solve for the wet coil a method proposed by Elmahdy and Mitalas (1977) was implemented in which an enthalpy exchanger was used to solve for the total heat and mass transfer. This method solved for the sensible and latent portions of the coil simultaneously. The exiting air state and total heat transfer was calculated by using the entering air enthalpy and the enthalpy of the cold stream at the surface temperature of the entering water stream. The enthalpy of the exiting air stream was used to determine the total heat transfer on the airside. The humidity ratio of the exiting air was then determined by iteration since the temperature and enthalpy are known.

Based on the previous body of literature it is evident that the outcome of every research topic was to produce either a computationally efficient steady state model, or a more accurate time variant model. Many of the models proposed in the previous literature were validated against either previous models or against slightly more complex numerical versions of the same model.

# 3 Methodology

## 3.1 – Matlab Simulink Simulation Tool

The first priority of this research was to develop a simulation tool in an environment that would allow for coil characteristics to be changed as well as visual way to display results. Matlab Simulink was chosen for its robust visual programming environment as well as its ability to produce high-quality plots. In order to investigate how heat transfer rates are affected by changing input parameters, a cooling coil model that accounts for both latent and sensible heat transfer was built. It is a difficult task to solve differential equations across the entire coil due to the complex heat transfer that occurs in a crossflow fin tube heat exchanger. The addition of latent heat transfer also makes the problem more difficult. It was important to build the model in a way which would give the user the ability to change not only the size and construction of the coil but also the input parameters and geographic location of the coil. This allowed for a single model to be built that then easily could be calibrated to any real system.

The model is broken down into multiple sections. The first section calculates the coil geometry and heat transfer coefficients on both the waterside and airside. Depending on the conditions of the entering air and water, the information from the first section is used to calculate the fin efficiency and the overall heat transfer coefficient for either a dry or wet coil. Those calculations are then passed to either the sensible or latent portion of the coil model to calculate exit conditions and heat transfer rates. The effectiveness-number of transfer unit's method for a heat exchanger is used in the sensible portion of the model with some assumptions to simplify the complex differential equations that actually describe heat transfer rates. The latent portion of the model includes mass transfer due to the dehumidifying affect when moist air comes in contact with the cold coils. In this case a modified effectiveness-NTU method is used in an enthalpy exchanger to account for heat and mass transfer on the airside. To reduce the computation time of the simulation, the partially wet case was not represented in the model.

## 3.2 – Data Acquisition and Experimental Study

A well-known European manufacturer of actuators and control valves has partnered with the University of Colorado and MIT to test their new control valve in hopes to mitigate the low delta-T syndrome experienced in the IMIG Music building and Hayden Library respectively. The control

valves they installed at both locations have a water flow sensor, and two sensors to measure supply water and return water temperatures. The valves also have an intelligent actuator, which holds the control logic while receiving a signal from the DDC system. What makes this product special is that it also can receive firmware updates via an Ethernet cable, which allow for constant updates to its control logic. For the purpose of this test only, airside sensors placed in the duct, up and down stream of the coil will also gather data to be analyzed. Six valves were installed at MIT and five valves were installed at CU.

The MIT valves began gathering data in July while the valves at CU campus took considerably longer to configure due to the security of the campus IT department. The valves at CU began gathering useable data in September, although because the cooling demand was not at peak the data was only used for calibration purposes. The data acquired at MIT on the other hand was more pertinent for the purpose of developing control strategies because it provided insight into the performance of the coil and valve during the season with the highest cooling demand. The data acquisition portion of the research was critical to the success of the project, although the acquisition process proved to be a difficult task due to the security protocols of both campus networks. In order to remotely access the data acquired from each actuator strict security measures were taken. A large amount of data has been gathered from MIT and CU and is used in conjunction with the Simulink model to validate and develop control strategies for the new actuator. This combination of computer simulation with actual field data allows for a unique investigation into the behavior of cooling coils in operation.

### 3.3 – Model Calibration

Using the data collected at MIT and CU Boulder the Simulink model was calibrated so it reflected the same properties as the actual coils used in both air-handling units. It was determined to use data from two locations to better understand how the coil behaves for both sensible and latent heat transfer mechanisms. Data collected from test units (Figure 1 and Figure 2) were used as input for the computer simulation. These variables include supply water temperature, water flow rate, airflow rate, humidity, and mixed air temperature. The simulation output was compared with the actual field data and the results were then used to further tune the mode. The calibration step is important because it validates the computer model and allows for confidant interpretation of future results.

**Figure 1 - MITs AHU-6 coil detail**

**Figure 2 - CUs AHU-1**

## 3.4 – Control Logic Strategy Development

Once calibrated, the Simulink model can be used as a tool to investigate heat transfer rates under various supply conditions. Various simulations are conducted to visually document how the performance of the coil is affected by the changing input parameters. The results from this

investigation will be used to inform the control logic strategy developed for the initial release of the new valve type. The initial release of the control valve and actuator will contain logic that will maximize delta-T, preventing it from dropping too low. Further releases of the logic will have improvements based on recommendations from this research.

# 4 Model Development

## 4.1 – Modeling Software

Matlab Simulink modeling software was chosen for its robust programming user interface and its ability to render meaningful engineering plots with ease. The program has the ability to be compiled into C+ code for use in future simulations. Model calibration with actual data was a much simpler task due in part to Simulink's ability to plot signals along every path of the model. This was crucial in helping to visualize how heat transfer rates varied with changing input parameters.

## 4.2 – Problem Statement

After conducting the previous research it was determined that a steady state modeling approach would be both computationally efficient and accurate enough to simulate heat transfer rates and exiting fluid states for a typical counter cross-flow, plat-fin-tube cooling coil. The target of this model is to calculate heat transfer rates over longer time periods such as a few weeks to a month;

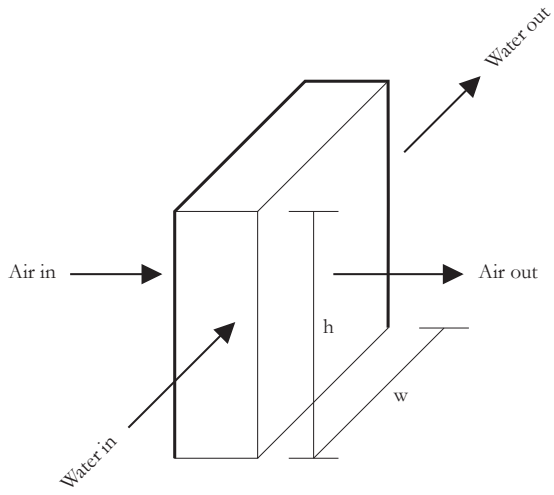


**Figure 3 – Counter cross-flow coil configuration**

therefore a second-by-second analysis is not necessary as with the dynamic modeling approach. Dynamic models are often used for the development of advanced feedback controllers in which a time variant solution is necessary. Figure 3 depicts the basic dimensions and flow direction of the hot and cold fluids where *w* is the coil width and *h* is the coil height. The model has been developed in such a way that specific coil dimensions can be entered before the start of the simulation to accurately represent various coil sizes. In this configuration, hot air enters the coil parallel to the fins and perpendicular to the water tubes, while water enters the coil on the air-out side and exits the coil

on the air-in side. This allows for the most efficient heat transfer between the two unmixed fluids in a counter cross-flow configuration. Figure 4 illustrates the flow of fluids across the fins and tubs. The model has been developed to solve for both the sensible and latent heat transfer mechanisms that occur in a dehumidifying cooling coil, although some assumptions have been made to greatly simplify the calculations involved:

- Water and air are incompressible
- Ideal gas relationships for air and water vapor
- Uniform velocity of air across the coil between the fins
- Bends in tubes have been neglected
- Partially wet coil scenario has been neglected
- Water temperature degradation at discrete intervals is not calculated
- Uniform densities of coil material

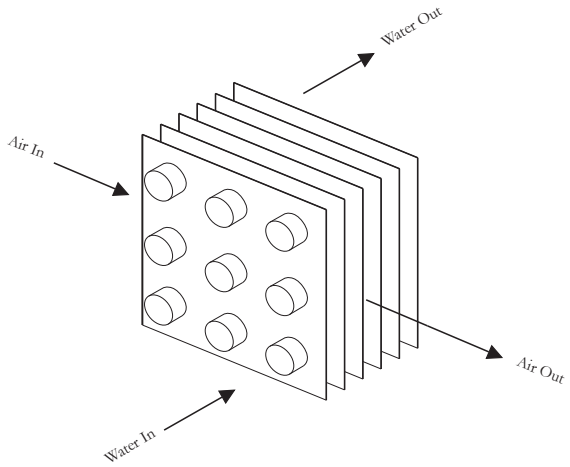


**Figure 4 - Rectangular tube array and fin spacing diagram**

## 4.3 – Input, Output and Static Variables

The following list of parameters are entered at the beginning of the simulation and are considered static values used for internal calculations:

Coil Type
0 = Flat fins; 1 = Circular fins
Outside diameter of tube (m)
Width of coil (m)
Height of coil (m)
$\delta$ – Fin thickness (m)

Row spacing (m)
Tubes per row
Minimum air flow area/face area
$D_{h,pipe}$ – Inside diameter of tube (m)
$D_{o,pipe}$ – Outside diameter of tube (m)
$R_f$ – Fouling factor $\left(\frac{Cm^2}{W}\right)$

Number of rows of tubes
$k_{tube}$ –Tube thermal conductivity $\left(\frac{W}{mC}\right)$
Number of circuits
$P_{atm}$ –Atmospheric pressure (Pa)
$C_{P,L}$ – Liquid specific heat $\left(\frac{J}{KgK}\right)$

$C_{P,vap}$ – Sat vapor specific heat $\left(\frac{J}{KgK}\right)$

$k_L$ –Liquid thermal conductivity $\left(\frac{W}{mC}\right)$

$\mu_L$ –Liquid dynamic viscosity $\left(\frac{Kg}{ms}\right)$

$k_{fin}$ –Fin thermal conductivity $\left(\frac{W}{mC}\right)$

$f_s$ – Fin spacing (m)

$\mu_{air}$ – Air dynamic viscosity $\left(\frac{Kg}{ms}\right)$

Fins per meter $\left(\frac{1}{m}\right)$

$C_{P,d-air}$ – Dry air specific heat $\left(\frac{J}{KgK}\right)$

$k_{air}$ –Air thermal conductivity $\left(\frac{W}{mC}\right)$

The input parameters for the model are air mass flow $(\dot{m}_{air})$, air temperature $(T_{air,in})$, relative humidity $(RH)$, water mass flow $(\dot{m}_L)$, and water temperature $(T_{water,in})$. The output variables the model solves for are air temperature $(T_{air,out})$, humidity ratio $(HR)$, water temperature $(T_{water,out})$, air enthalpy $(h_{air,out})$, total $(\dot{Q}_T)$, sensible $(\dot{Q}_S)$, and water-side $(\dot{Q}_W)$ heat transfer rates.

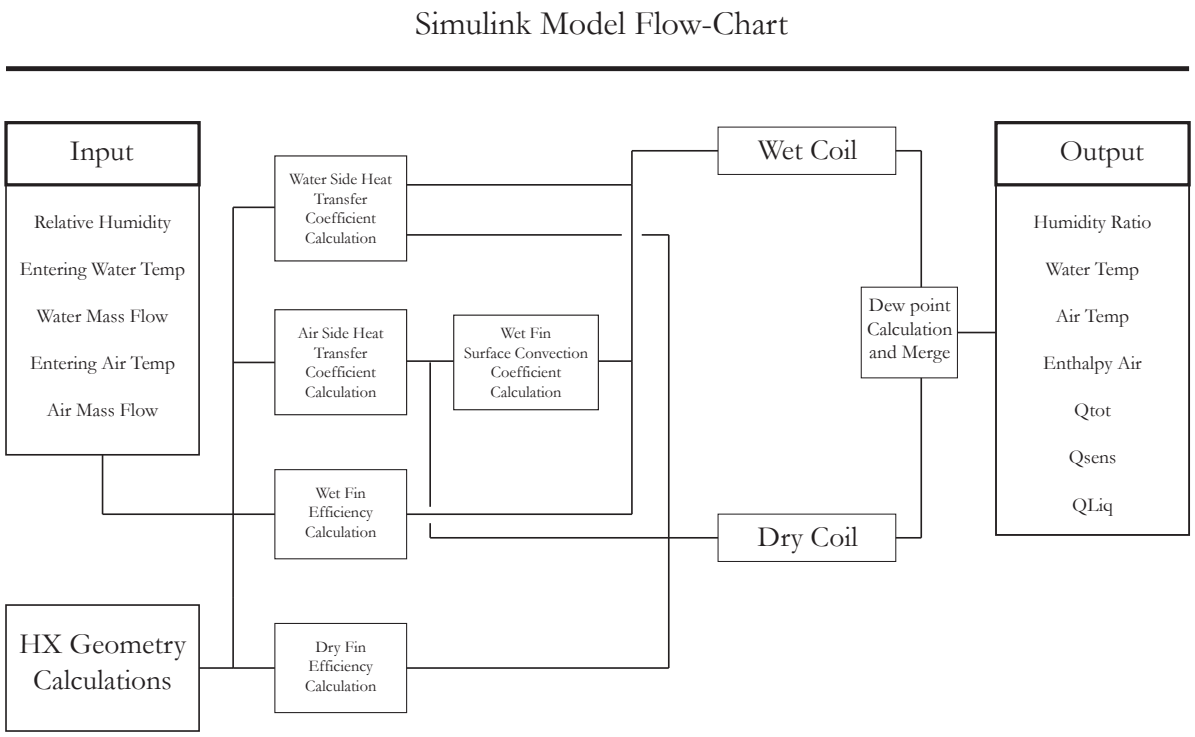


**Figure 5 - Simulink model calculation flow chart**

## 4.4 – Modeling Approach

As shown in Figure 5, the model is split into eight effective categories; input variables, heat exchanger geometry calculations, heat transfer coefficient calculations, fin efficiency calculations, wet coil model, dry coil model, dew point calculation and output variables. In a typical cooling coil there will be dehumidification if the dew point of the entering air is greater then the surface temperature

of the entering water tube. In this case there will be energy removed from the airside in the form of condensation on the coil surface. In order to effectively simulate this scenario the model has two major components, which separate the sensible and latent calculations into two blocks. The core structure of the model is based on the classical effectiveness-NTU method, which solves for the sensible portion, and an enthalpy based approach, which is used to solve for the latent portion of the model. When the dew point of the air is less then the entering water temperature only the sensible portion of the model is activated and visa versa. The model if further simplified by calculating an overall UA for both the sensible and latent portions where UA is defined as a function of waterside resistance, conduction resistance, airside resistance and fouling factor resistance.

$$\frac{1}{UA} = \frac{1}{h_f A_a \eta_f} + \frac{\Delta x}{k_{tube} A_m} + \frac{1}{h_{int} A_{int}} + R_f \tag{2}$$

Heat transfer on the waterside is based on the overall UA described in Equation 2 and can be defined as

$$\dot{Q} = UA(T_{co} - T_{ci}) \tag{3}$$

where $T_{co}$ and $T_{ci}$ are the exit and inlet water temperatures respectively. Because of this simplification discrete temperature profiles within the coil are not calculated. The simulation starts with heat exchanger geometry calculations, which are only made once. These values are then passed on to calculate the water and airside heat transfer coefficients as well as fin efficiency for both the wet and dry coil cases. Finally, an overall UA is calculated and passed to either the dry or wet coil blocks. During this process a dew point calculation is made to determine whether there is dehumidification within the coil. Based on this calculation, either a sensible or latent heat transfer value is then passed on as an output.

### 4.5 – Initial Parameter Calculations

Initial parameter calculations for heat transfer areas and HX geometry are done in a separate block at the beginning of the simulation. Before the simulation starts it is necessary to define material properties and coil geometry on both the waterside and airside portions of the heat exchanger as shown in Figure 6. For the purpose of this research the model developed is based on two cooling coils; AHU1 in CUs IMIG music building and AHU-6 in MITs Hayden Library, in which actual water and airside data is remotely collected for the purpose of model calibration. This

allows for a model to be developed and calibrated to an actual cooling coil in operation in both a dry and humid climate, which allows for more accurate simulation results. Data at both locations was used to calibrate the model for both a mostly dry scenario and a wet-coil scenario. The humidity levels are so low in Boulder that the coil experiences sensible heat transfer the majority of operating hours. In this case the dewpoint temperature of the entering air is less then the temperature of the supply water. Boston on the other hand experiences dewpoint temperatures of the entering air that are higher then the entering water temperature, therefore dehumidification will occur within the coil activating the latent heat transfer blocks. Visual inspection of both coils yielded an estimate for the dimensions, although because of the difficult access to the coils there is some uncertainty in the exact parameters of each coil. AHU-1 at CU Boulder is estimated at 2 meters high by 2.3 meters wide with 30 tubes per row, 380 fins per meter and 8 rows of tubes. AHU-6 at MIT is 2 meters wide by 1.5 meters high, with 34 tubes per row, 8 rows of tubes and 354 fins per meter. The initial parameters are entered in the model for the first simulation. The calibration process will be described in detail in a later portion of this research, which will include tuning the model for variations in the uncertain parameters. Nominal calculations are made during this phase of the simulation in which waterside and airside heat transfer areas are calculated using the geometry inputs. The following list of parameter values are also used for further calculations within the model:

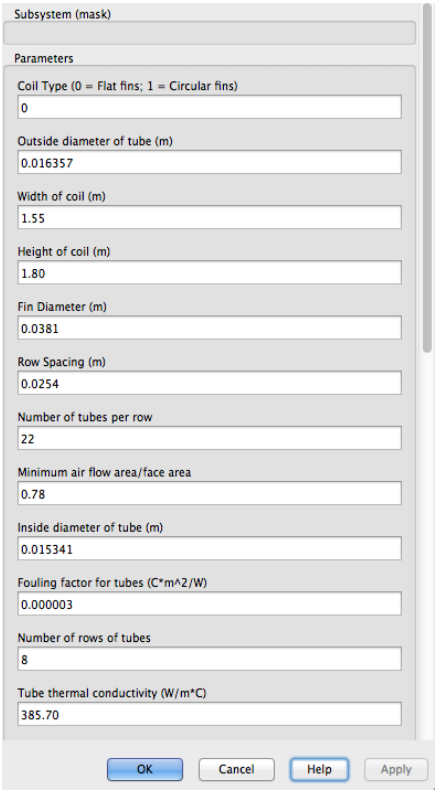


**Figure 6 - Parameter input example**

- Outside diameter of tube (m) - 0.016357
- Fin diameter (m) – 0.0381
- Row spacing (m) – 0.0254
- Inside diameter of tube (m) - 0.015341
- Fouling factor ($C*m^2/W$) – 0.000003
- Copper tube thermal conductivity (W/m*C) – 385.70
- Number of circuits – 8
- Atmospheric pressure (Pa) – 101325
- Liquid specific heat (J/kg*C) – 4186
- Liquid thermal conductivity (W/m*C) – 0.604
- Liquid dynamic viscosity (kg/m*s) – 0.00144
- Fin thermal conductivity (W/m*C) – 228.30

- Fin thickness (m) – 0.0001905
- Air dynamic viscosity (kg/m*s) - 0.0000182
- Dry air specific heat (J/kg*C) – 1006
- Air thermal conductivity (W/m*C) – 0.026
- Water vapor specific heat (J/kg*C) – 1805
- Latent heat of vaporization (J/kg) – 2501000

The previous properties used in the simulation are taken from Cengel and Boles (2008).

## 4.6 – Heat Transfer Coefficient Calculations

Heat transfer coefficients are calculated on the waterside and airside for both the dry and wet coil cases by using classical empirical relationships developed in previous research. On the waterside heat transfer occurs between the water and the pipe wall by the way of convection and conduction. The heat transfer coefficient is defined as

$$h_{int} = \frac{Nuk_L}{D_{h,pipe}} \tag{4}$$

where $Nu$ is the Nusselt number, $k_L$ is the fluid thermal conductivity and $D_{h,pipe}$ is the hydraulic diameter of the pipe (ASHRAE 2009). Fluid flow through pipes can be categorized into three regimes, laminar, turbulent, and transitional, each of which are a function of the dimensionless Reynolds number, defined as

$$Re = \frac{\phi_L D_{h,pipe}}{\mu} \tag{5}$$

in which $\phi_L$ is the mass flux liquid and $\mu_L$ is the dynamic viscosity of the fluid at the wall defined as 93% of the bulk dynamic viscosity (Brandemuehl et al. 1993). Flow is considered turbulent when the Re number is greater then 4000 and laminar when less then 2300 (ASHRAE 2009). Empirical relationships for heat transfer coefficients inside tubes are described in ASHRAE (2009) and are based on the research by Seider and Tate (1936) in which the Nusselt number is defined as

$$Nu = (1.86RePrD_h/L)^{0.333}(\mu_b/\mu_w)^{0.14} \tag{6}$$

for laminar flow and

$$Nu = (0.027Re)^{0.8}Pr^{0.333}(\mu_b/\mu_w)^{0.14} \tag{7}$$

for turbulent flow. The Prandtl number is defined as

$$Pr = \frac{\mu_L C_{p,L}}{k_L} \tag{8}$$

where $C_{p,L}$ is the specific heat of the fluid in question. Transitional flow regime is defined using a difference approximation between the laminar and turbulent Nusselt numbers (Brandemuehl et al. 1993). Finally, the heat transfer coefficient $h_{int}$ in Equation 2 is solved using either the turbulent, laminar or transitional relationships.

The convection coefficient on the airside is calculated as a function of the Reynolds, Prandtl number and the dimensionless j-factor proposed by Chilton and Colburn (1934). The j-factor describes the heat transfer on the airside when considering fin-tube configurations and can be defined as

$$J = \left(\frac{h_{f,dry}}{\phi_A C_{P,d-air}}\right) Pr^{2/3} \tag{9}$$

where $h_{f,dry}$ is the convection coefficient of the air, $\phi_A$ is the mass flux of the air through the coil and $C_{P,d-air}$ is the specific heat of the dry air. The empirical relationship used in this model for the j-factor as a function of the Reynolds number has been developed by (D. H. Elmahdy 1979) and can be defined as

$$J = C_1 Re^{C_2} \tag{10}$$

where the coefficients $C_1$ and $C_2$ are determined numerically as a function of fin thickness, fin spacing, fin height, fin diameter, tube diameter and tube spacing. The coefficients $C_1$ and $C_2$ are defined as

$$C_1 = 0.159 \left(\frac{\delta}{f_h}\right)^{0.0141} \left(\frac{D_{h,coil}}{\delta}\right)^{0.065} \tag{11}$$

and

$$C_2 = -0.323 \left(\frac{\delta}{f_h}\right)^{0.049} \left(\frac{f_s}{\delta}\right)^{0.077} \tag{12}$$

in which $\delta$ is the fin thickness, $f_h$ is the fin height and $f_s$ is the fin spacing. The heat transfer coefficient $h_{f,dry}$ on the airside is then solved as a function of Equation 8, mass flux air and air specific heat.

A similar relation was developed by Kraus et al. (2001) for estimating the heat transfer coefficient $h_{f,wet}$ for the wet coil case and is defined as:

$$h_{f,wet} = 0.231(Re)^{0.69}\left(\frac{k_{air}}{D_{h,coil}}\right) \tag{13}$$

## 4.7 – Fin Efficiency Calculations

The fins within the coil aid in the heat transfer between the hot and cold fluids by increasing the heat transfer area in question. Because the fins do not have a uniform temperature profile a fin efficiency $\eta$ is used to describe the heat-transfer rate where $\eta$ is defined as the ratio of actual heat transfer of the fin and base to the heat transfer of the fin and base at the base temperature of the fin. Effective fin efficiency is used in Equation 2 to define the airside resistance

$$R_a = \frac{1}{h_f A_a \eta_f} \tag{14}$$

where $h_f$ is the heat transfer coefficient on the airside, $A_a$ is the airside heat transfer area, and $\eta_f$ is the efficiency of either the dry or wet fin. Consider the rectangular tube array of Figure 7 in which

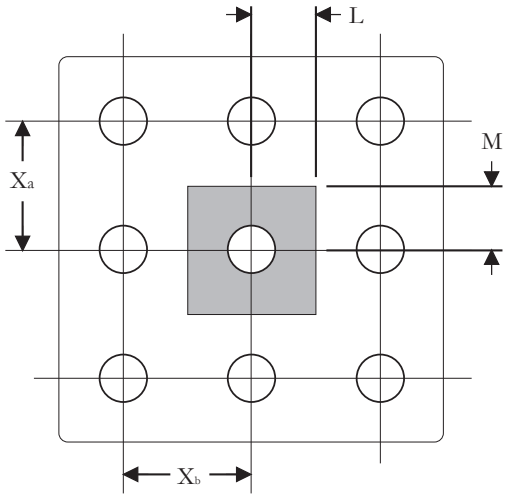


**Figure 7 - Rectangular tube array**

the heat transfer coefficient is considered to be constant over the whole fin surface (McQuiston, Parker and Spitler 2005). An empirical method for calculating fin efficiency, based on rectangular tube array geometry is validated by Schmidt (1945) and is summarized as follows:

$$\eta_{f,dry} = \frac{tanh(mr\phi)}{mr\phi} \tag{15}$$

where $r$ is the radius of the outside of the tube and $m$ is

$$m = \sqrt{\frac{2h_{f,dry}}{k_{fin}\delta}} \tag{16}$$

where $k_{fin}$ is the fin thermal conductivity and $\phi$ is defined as

$$\phi = \left[\left(\frac{r_e}{r}\right) - 1\right]\left[1 + 0.35ln\left(\frac{r_e}{r}\right)\right] \tag{17}$$

The value of $\frac{r_e}{r}$ can be found using the dimensions of the tube array geometry shown in Figure 7 and is defined as follows (Schmidt 1945):

$$\frac{r_e}{r} = 1.27\psi\sqrt{\beta - 0.3} \tag{18}$$

where $\psi$ is

$$\psi = \frac{X_a/2}{r} \tag{19}$$

and $\beta$ is defined as

$$\beta = \frac{X_b/2}{X_a/2}. \tag{20}$$

In Equation 19 and 20 the coefficient $X_b$ is the row spacing while the coefficient $X_a$ is determined during the initial parameter calculations as a function of the number of tubes per row and the coil height. The wet fin efficiency calculations are carried out exactly as the dry fin case. Although fin

efficiency does decrease when condensation occurs (Elmahdy and Biggs 1983), the effect is negligible for the purpose of this model and is therefore neglected.

## 4.8 – Dry Coil Method

The dry coil case employs the classical effectiveness-NTU method in which the parameter NTU (number of transfer units) can be thought of as a heat-transfer size factor (McQuiston, Parker and Spitler 2005). This method defines the effectiveness $(\varepsilon)$ of the cooling coil as the ratio of the actual heat transfer rate to the maximum possible heat transfer rate that the coil can achieve given the parameters and input variables.

$$\varepsilon = \frac{Actual\ heat\ transfer\ rate}{Maximum\ possible\ heat\ transfer\ rate} \tag{21}$$

The actual heat transfer rate is defined as

$$\dot{Q} = C_h(T_{hi} - T_{ho}) = C_c(T_{co} - T_{ci}) \tag{22}$$

where $C_h$ is the capacity of the air, $T_{hi}$ is the mixed air temperature, $T_{ho}$ is the supply air temperature, $C_c$ is the capacity of the water, $T_{ci}$ is the supply water temperature, and $T_{co}$ is the return water temperature. The maximum possible heat transfer rate would occur if one of the fluids were to undergo a temperature change equal to the maximum in the cooling coil, which would be equal to the temperature difference between the entering air and water (ASHRAE 2009). The maximum possible heat transfer rate is therefore

$$\dot{Q}_{max} = C_{min}\left(T_{h,in} - T_{c,in}\right) \tag{23}$$

where $C_{min} = \dot{m}_{min}C_{p,min}$ is the minimum capacitance of either the hot or cold fluid. Defined in terms of effectiveness the actual heat transfer rate is

$$\dot{Q} = \varepsilon\dot{Q}_{max} \tag{24}$$

Effectiveness relationships have been developed by previous researchers, which empirically describe the heat transfer rate for various heat exchanger configurations (ASHRAE 2009). The effectiveness of the cross flow coil where both fluid streams are unmixed is defined as

$$\varepsilon = 1 - exp\left\{\frac{1}{\eta C^*}\{exp[(-Ntu)\eta C^*] - 1\}\right\} \tag{25}$$

where the coefficient $\eta$ is

$$\eta = Ntu^{-0.22} \tag{26}$$

,$Ntu$ is

$$Ntu = \frac{UA}{C_{min}} \tag{27}$$

and $C^*$ is the capacitance ratio defined as

$$C^* = \frac{C_{min}}{C_{max}} \tag{28}$$

In order to solve for Equation 25 the overall $UA$ must be calculated by using Equation 2, which defines $UA$ as a function of the airside, waterside, conduction and fouling resistances. The following equation can now be used to solve for the exiting fluid states:

$$\dot{Q} = C_h(T_{hi} - T_{ho}) = C_c(T_{co} - T_{ci}) \tag{29}$$

Rearranging the terms to solve for the supply air temperature and the return water temperature yields:

$$T_{ho} = T_{hi} - \frac{\varepsilon \dot{Q}_{max}}{C_h} \tag{30}$$

and

$$T_{co} = T_{ci} + \frac{\varepsilon \dot{Q}_{max}}{C_c} \tag{31}$$

respectively.

Because this is the dry coil scenario, the exiting air humidity ratio is be equal to the inlet states since there is no mass transfer from the dehumidification process. For use in both the dry and wet coil cases, the entering air humidity ratio and enthalpy are calculated using psychrometric equations. The humidity ratio (*HR)* defines the mass of moisture in the air per unit mass of air and typically has units $\frac{kg}{kg}$. HR is a function of the mixed air temperature, relative humidity and atmospheric pressure and is defined as

$$g_o = \frac{0.62198 * P_w}{P_{atm} - P_w} \tag{32}$$

where $P_{atm}$ is the local atmospheric pressure and $P_w$ is the vapor pressure. In order to calculate the HR at a specific temperature and relative humidity, the saturated vapor pressure must be calculated using the following equation:

$$P_{ws} = e^{\left(\frac{C8}{T} + C9 + C10T + C11T^2 C12T^3 + C13ln(T)\right)} \tag{33}$$

where the coefficients $C8$ to $C13$ (ASHRAE 2009) are

$$C8 = -5.8002206e3$$
$$C9 = 1.3914993e0$$
$$C10 = -4.8640239e - 02$$
$$C11 = 4.1764768e - 05$$
$$C12 = -1.4452093e - 08$$
$$C13 = 6.5459673e0$$

The vapor pressure $P_w$ is then calculated by multiplying Equation 33 with the relative humidity of the mixed air and is then used in Equation 32 to solve for the humidity ratio of the entering air.

The enthalpy of the entering air can then be calculated by using the following equation (ASHRAE 2009):

$$h_{air,in} = l_v + C_{P,vap} T_{hi} w_{air,in} + C_{P,d-air} T_{hi} \tag{34}$$

where $l_v$ is the latent heat of vaporization of water, $C_{P,vap}$ is the specific heat of water vapor (Cengel and Boles 2008) and $w_{air,in}$ is the humidity ratio calculated in Equation 32.

## 4.9 – Wet Coil Method

In order to determine whether the dry or wet coil blocks of the model should be executed, a comparison is made between the dew point temperature of the mixed air and the temperature of the coil surface. The coil surface temperature is taken to be the temperature of the supply water. When the dew point temperature of the entering air is less then the supply water temperature the dry coil portion of the model is executed. If this comparison is false there will be dehumidification within the coil thus executing the wet coil portion of the model. Because of dehumidification within the coil there will be mass transfer from the moist air to the coil in the form of condensation on the coil surface. In this case it is considered that the coil is completely wet. In order to solve for the exiting fluid states an enthalpy-based approach to the effectiveness-NTU model is employed.

The dew point temperature is calculated as a function of atmospheric pressure and humidity ratio of the entering air and is defined by the following equation (ASHRAE 2009):

$$T_{dp} = -\left(\frac{424-\frac{7248}{15.463-ln\left(\frac{1}{3.376P_w}\right)}}{1.8}\right) \tag{35}$$

where $P_w$ is the vapor pressure of the air given by

$$P_w = \frac{w_{air,in}P_{atm}}{0.62198+w_{air,in}} \tag{36}$$

Once it is determined that the wet coil block is executed, an approach developed by Elmahdy and Mitalas (1977) is employed in which the effectiveness-NTU method is modified. The enthalpy based approach uses equivalent enthalpies in the heat exchanger model described in the dry coil case. In this the coolant stream in the sensible case is replaced by and equivalent saturated enthalpy of the air at the temperature of the supply water. In order to define the heat transfer rate using the enthalpy approach the overall UA value needs to be manipulated slightly. According to the research conducted by Elmahdy and Mitalas (1977) an equivalent UA is calculated as follows:

$$UA_h{}^* = \frac{1}{\frac{C_p{}^*}{UA_{int}} + \frac{C_{P,air}}{UA_{ext}}} \tag{37}$$

in which the capacitance on the waterside is replaced with an equivalent capacitance based on an enthalpy difference between the enthalpy of the air at the dew point temperature and the saturated enthalpy of the air at the supply water temperature. In Equation 36 the specific heat $C_p{}^*$ of the air at the entering water temperature is defined as

$$C_p{}^* = \frac{h_{a,dp} - h_{a,L,in}}{T_{dp} - T_{L,in}} \tag{38}$$

where $h_{a,dp}$ is the enthalpy of the mixed air at the dew point temperature, $h_{a,L,in}$ is the saturated enthalpy of the air at the temperature of the supply water, $T_{dp}$ is the dew point temperature of the entering air, and $T_{L,in}$ is the temperature of the supply water. The overall UA on the waterside is calculated as

$$UA_{int} = \frac{1}{R_f} + h_{int}A_{int} \tag{39}$$

while the overall UA on the airside is

$$UA_{ext} = h_f A_a \eta_f \tag{40}$$

Equation 38, 39, and 40 are used in Equation 37 to solve for the overall UA of the wet coil scenario. Once the overall UA is calculated a modified effectiveness-NTU method is employed to calculate the enthalpy of the supply air. The effectiveness is defined according to a modified Equation 21 and is as follows:

$$\varepsilon^* = \frac{(h_{air,in} - h_{air,out})}{(h_{air,in} - h_{sat,air,L,in})} = \frac{\dot{Q}}{\dot{Q}_{max}} \tag{41}$$

with an actual heat transfer rate of

$$\dot{Q} = \dot{m}_{air}\left(h_{air,in} - h_{air,out}\right) = \dot{m}_{air}\left(h_{sat,air,L,in} - h_{sat,air,L,out}\right) \tag{42}$$

In this relationship equivalent enthalpies are calculated. $h_{sat,air,L,in}$ is the saturated enthalpy of air at the supply water temperature and $h_{sat,air,L,out}$ is the saturated enthalpy of air at the return water temperature (ASHRAE 2009) (Elmahdy and Mitalas 1977). Mass transfer effectiveness is based on airside enthalpies. Analogous to the dry coil case, it is the ratio of the actual enthalpy change to the maximum change. The maximum change would occur if the air leaving the coil were at the same temperature of the water entering the coil. In other words the enthalpy of the air leaving the coil would have to be the saturated enthalpy of air at the entering water temperature. The maximum heat transfer rate can then be defined as

$$\dot{Q}_{max} = \dot{m}_{air}\left(h_{air,in} - h_{sat,air,L,in}\right) \tag{43}$$

Similar to the dry coil case the effectiveness (ASHRAE 2009) of a cross-flow heat exchanger of a wet coil can be defined as

$$\varepsilon^* = 1 - exp\left\{\frac{1}{\eta {C_h}^*}\{exp[(-Ntu^*)\eta {C_h}^*] - 1\}\right\} \tag{44}$$

with some modification of the capacitance ratio ${C_h}^*$ and the value of $Ntu^*$. Both of these values are redefined based on Equation 38 and are as follows:

$${C_h}^* = \frac{\dot{m}_{air}{c_p}^*}{\dot{m}_L c_{P,L}} \tag{45}$$

$$Ntu^* = \frac{U{A_h}^*}{\dot{m}_{air}} \tag{46}$$

$$\eta = {Ntu^*}^{-0.22} \tag{47}$$

The enthalpy of the supply air and total heat transfer is then solved using Equation 41 and Equation 42 respectively. Next, we determine the other exit states by using a temperature effectiveness relation and by calculating the temperature of the condensate. It is noted that in this case the minimum capacitance is the entering air stream and the max capacitance is the condensate itself. In this case the C-ratio $\frac{C_{min}}{C_{max}}$ goes to zero. This happens when one fluid undergoes a phase change and

the capacitance goes to infinity (Elmahdy and Mitalas 1977) (Brandemuehl et al. 1993). The specific heat of the moist air is defined as

$$C_{P,m-air} = \dot{m}_{air}\left(C_{P,air} + w_{air,in}C_{P,vap}\right) \tag{48}$$

Again the same relation for enthalpy effectiveness is used, with substitution of the enthalpy at the temperature of the condensate, and is defined as

$$\varepsilon = \frac{(h_{air,in} - h_{air,out})}{(h_{air,in} - h_{air,cond,in})} \tag{49}$$

with $\varepsilon$ defined as

$$\varepsilon = 1 - e^{-Ntu} \tag{50}$$

and

$$Ntu = \frac{(UA_{ext})}{(C_{P,m-air})} \tag{51}$$

The temperature of the condensate is then calculated by using the saturated air enthalpy as a point on the psychrometric chart. The temperature of the condensate must be solved using iteration by initially guessing at a temperature, calculating the enthalpy then minimizing the error between the guess and the enthalpy of the condensate (Figure 8).

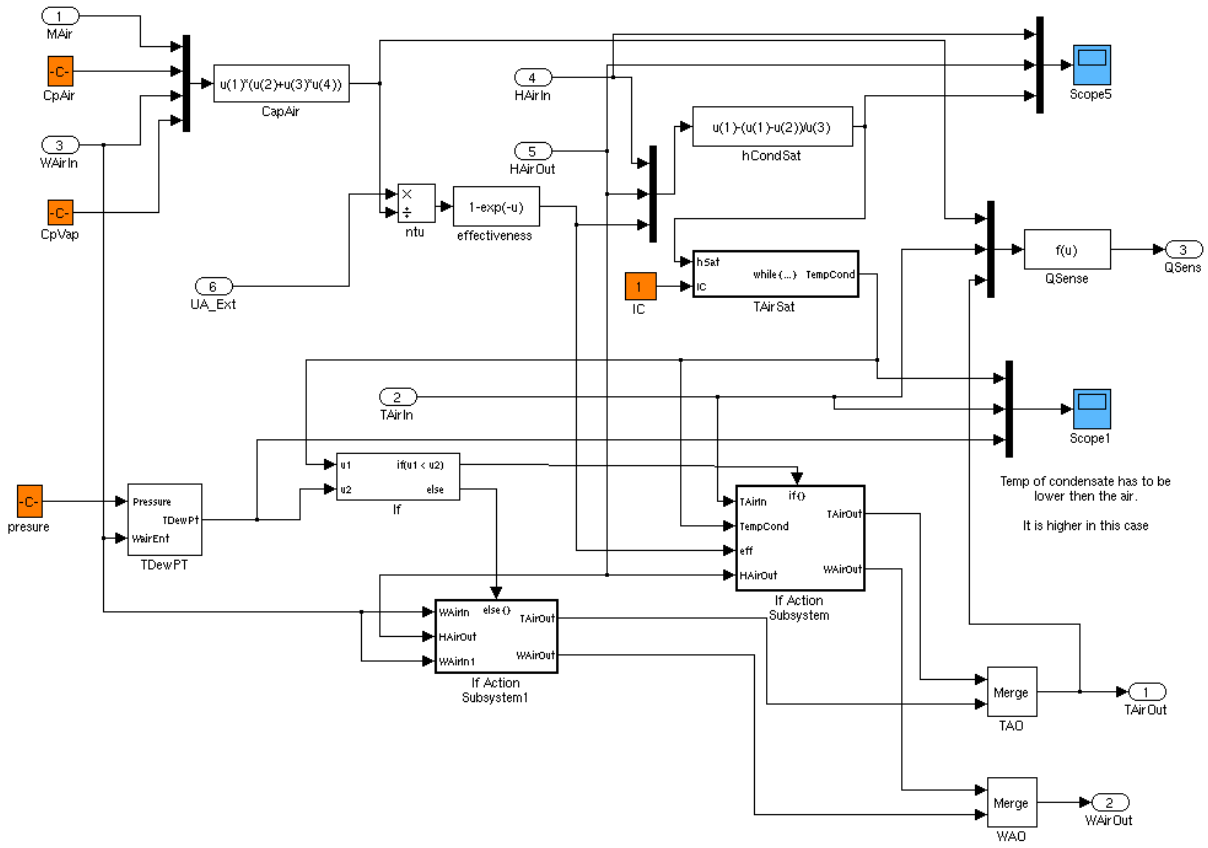


**Figure 8 - Iteration method to find the temperature of the condensate at a given enthalpy and pressure**

If the temperature of the condensate is less then the dew point temperature of the entering air, condensation will occur and there will be dehumidification of the air stream. The effectiveness relationship can then be used to calculate the exiting air temperature.

$$\varepsilon = \frac{(T_{air,in} - T_{air,out})}{(T_{air,in} - T_{air,cond,in})} \tag{52}$$

The humidity ratio of the exiting air can now be calculated by using the enthalpy and temperature of the exiting air. If the temperature of the condensate is greater then the entering air dew point temperature then there will be no dehumidification and the humidity ratio will remain the same as the entering condition. Sensible and total heat transfer can finally be calculated using the following relations

$$\dot{Q}_{sens} = \dot{m}_{air} C_{P,d-air} \left(T_{air,in} - T_{air,out}\right) \tag{53}$$

$$\dot{Q}_{tot} = \dot{m}_{air} \left(h_{air,in} - h_{air,out}\right) \tag{54}$$

# 5 Data Acquisition and Experimental Study

The data acquisition portion of the research was important because it enabled vast amounts of data to be acquired in order to calibrate the computer model to two actual cooling coils in operation. Without this data acquisition step the computer model would only be as valid as many of the previous models it is based off of. This experiment phase also allowed large amounts of data to be analyzed for the purpose of developing strategies to mitigate the low delta-T experienced across the hydronic circuit in question. The following section describes the installation and data acquisition process.

## 5.1 - Installation

In coordination with facilities maintenance and the valve manufacturer, six prototype ePIV valves were installed in MIT's Hayden library, while five ePIV valves were installed in CU Boulder's IMIG Music building. Both buildings experience a low chilled waterside temperature difference which results in increased pumping power. Facilities maintenance has had difficulty in trying to mitigate the low delta-T experienced in the buildings on both campuses. This presented the perfect opportunity to test the new control valves. The installation procedure involved a meticulous coordination between facilities maintenance, campus IT, contractors, and the valve manufacturer. The installation procedure was carefully orchestrated to ensure the highest level of security since each valve had to be connected to local area network of each campus as well as the building management system.

**Figure 9 - CU Boulder's IMIG Music building**

The IMIG Music building (Figure 9) is located 400 meters south of the central plant (Figure 10). The central plant is responsible for delivering steam to the building for heating. Chilled water is delivered directly to the air-handling units via a centrifugal chiller located in the mechanical room of

the building. Unlike Hayden library the IMIG music building maintains a relative humidity of 60% through the use of direct evaporative cooling. This is implemented due to the sensitivity of the instruments to low humidity levels. In order to maintain proper tuning of the pianos, humidity levels must not fall below this level. It should be noted that the Simulink model does not account for evaporative cooling and therefore the data acquired at CU is not used to calibrate the model.

MITs Hayden library (Figure 11) is located south east of the central plant (Figure 12) and is on


**Figure 10 - Map of CU Boulder's central plant and IMIG Music building**

**Figure 11 - MITs Hayden Library**

the end of the chilled water loop for the entire campus. In this case the central plant is responsible for delivering both steam and chilled water to Hayden library. Because Hayden library is on the end of the hydronic loop for the campus the chilled water temperature delivered to the building must

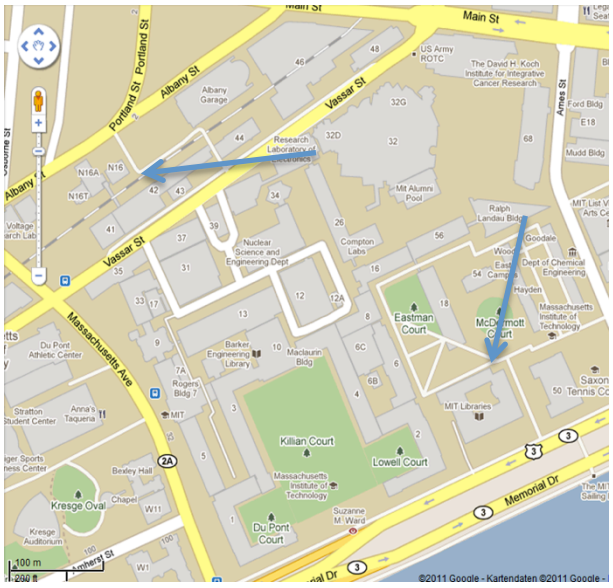


**Figure 12 - Map of MITs Hayden library and central plant**

**Figure 13 - Valve, actuator, and flow meter**

travel considerable distance. When cooling demand is high for the campus the temperature of the chilled water delivered to the building floats. The effects of this fluctuation is investigated in the next section of this research

Each valve installed (Figure 13) is equipped with a magnetic flow meter upstream of the valve, a supply and return water temperature sensor, and airside sensors that measure the enthalpy and temperature upstream and downstream of the cooling coil. Figure 16 shows the location of the new valve in the IMIG music building.

**Figure 16 - Valve location near CUs AHU-6**

An intelligent actuator that receives a signal from the building management system controls the valves. The actuator is assigned an IP address in which the settings can remotely be modified via any web browser. The connection is typically made directly to the local area network of each campus via a CAT 5 Ethernet cable although because of each campuses unique firewall, access to the valves had to be granted through a separate secure wireless connection. In order to overcome this problem access was granted through the use of separate netbook computers connected to each actuator. The basic configuration shown in Figure 13 illustrates the location of each valve and the connection to the building management system. For the purpose of this research two additional airside sensors were connected to each actuator. In order to accomplish this it was necessary to configure a test box in which the connections were routed through a separate node. The test box houses a router, power strip, and a node in which the actuator and remote sensors were connected. The basic configuration of the test box is seen in Figure 12. The test box also houses a netbook computer (not shown) in which the connection to the local network was made. A direct connection from the actuator to the node is made using an Ethernet cable. The netbook is then connected to the node and the router. Each campus provided a secure wireless portal to then remotely access the data recorded on the netbook. The actuator receives a signal from the building management system through MP-Bus communication. MP-Bus protocol is used to connect the actuator to the waterside temperature sensors. The node in the test box also receives a signal from the airside sensors via MP-Bus wiring. This node is then connected to the router, which is connected to the netbook. The wiring diagram of each actuator and test box is shown in Figure 17. Notice the connections to the DDC system, temperature sensors and power supply.

Once the valves were installed and connected they could then be accessed directly via any web browser through a secure web page. The commissioning process also took place via a web page in which characteristics of the valve were defined, including units, valve size, operation mode, altitude, water characteristics, and nominal flow rate of the water. Once the valve was in operation, the dynamic readings could be remotely viewed from the secure web page from anywhere in the world. This allowed for real time monitoring and adjustment of the valves as well as a way to update the firmware on the actuator.

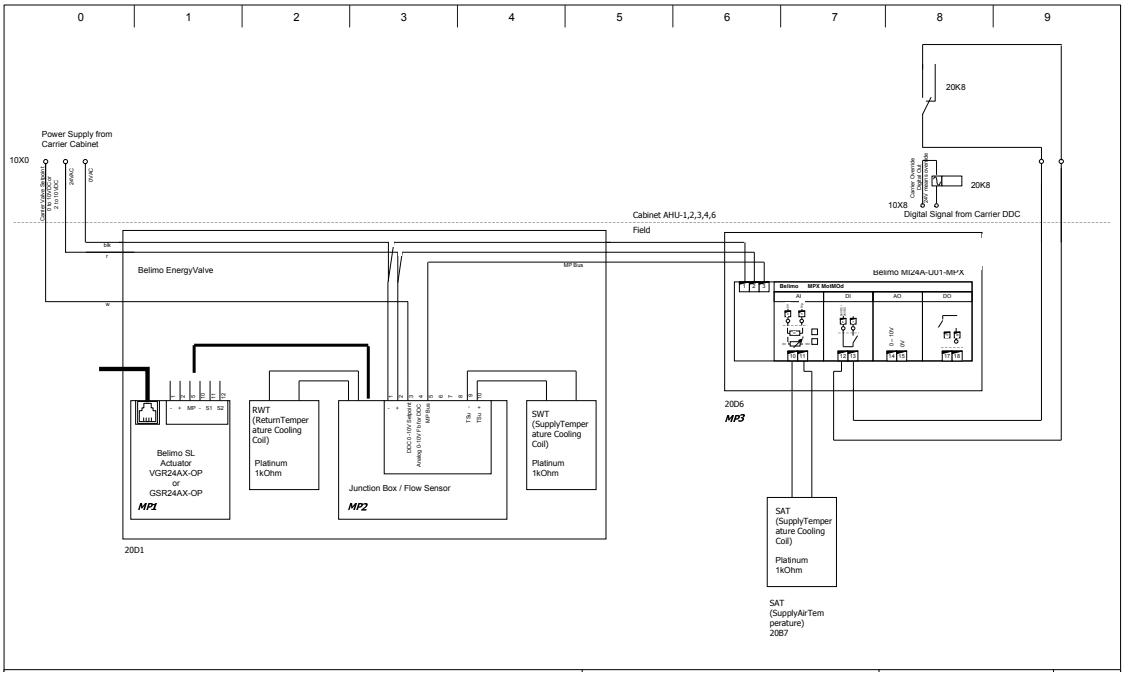


**Figure 17 - Wiring diagram for the actuator, test box, and remote sensors**

It should be noted that the installation and commissioning process took quite some time due to the security protocols of each campus. The valves at MIT began gathering data in June while the valves on CU Boulder's campus began gathering data in late August. For the purpose of this research it was necessary to use data from valves operating during the period with the highest cooling demand. Because of this only the MIT data was considered for this research. When looking at the data at CU Boulder it was evident that the coil was operating at part load since the cooling demand was low. The valves at CU Boulder are currently gathering data will eventually be analyzed once the cooling demand is high during the summer months.

## 5.2 – Remote Data Acquisition

The remote data acquisition portion of the research was essential to gain deeper insight into the dynamics of cooling coil operation. Once the installation and configuration procedure was complete, data was recorded and stored on each netbook for analysis purposes. Data is acquired and processed

**Table 1 - Output Example**

| Y | Fb % | V %ofVNom | V [GPM] | T1 [¡F] | T2 [¡F] | Pow2 [BTUH] | dT Abs [¡F] | Carrier Sp % | V-Sp % / Z(t) |
|---|---|---|---|---|---|---|---|---|---|
| 24.3 | 10.53 | 25.61 | 46.01 | 42.53 | 55.06 | 287800 | 12.53 | 24.21 | 34.22 |
| 24.12 | 10.48 | 25.41 | 45.64 | 42.52 | 55.04 | 285400 | 12.52 | 24.09 | 34.22 |
| 23.89 | 10.53 | 25.61 | 46.01 | 42.52 | 55.04 | 287800 | 12.53 | 23.82 | 34.22 |
| 23.25 | 10.35 | 24.8 | 44.55 | 42.57 | 55.08 | 278300 | 12.51 | 23.23 | 34.22 |
| 23.22 | 10.31 | 24.59 | 44.18 | 42.54 | 55.1 | 277100 | 12.56 | 23.24 | 34.22 |
| 22.92 | 10.31 | 24.59 | 44.18 | 42.57 | 55.29 | 280700 | 12.72 | 22.89 | 34.22 |
| 22.88 | 10.26 | 24.39 | 43.82 | 42.56 | 55.32 | 279200 | 12.76 | 22.87 | 34.22 |
| 22.25 | 10.13 | 23.78 | 42.72 | 42.6 | 55.37 | 272500 | 12.77 | 22.18 | 34.22 |
| 21.8 | 10.09 | 23.58 | 42.36 | 42.54 | 55.43 | 272600 | 12.89 | 21.71 | 34.22 |
| 21.72 | 9.87 | 22.56 | 40.53 | 42.53 | 55.59 | 264300 | 13.06 | 21.72 | 34.22 |
| 21.79 | 9.87 | 22.56 | 40.53 | 42.58 | 55.86 | 268800 | 13.28 | 21.75 | 34.22 |
| 21.31 | 9.87 | 22.56 | 40.53 | 42.6 | 56.05 | 272100 | 13.44 | 21.27 | 34.22 |
| 21.37 | 9.87 | 22.56 | 40.53 | 42.66 | 56.06 | 271300 | 13.4 | 21.37 | 34.22 |
| 21.03 | 9.78 | 22.16 | 39.8 | 42.7 | 56.07 | 265600 | 13.37 | 21 | 34.22 |
| 20.55 | 9.65 | 21.55 | 38.7 | 42.81 | 56.21 | 261500 | 13.4 | 20.57 | 34.22 |
| 20.05 | 9.56 | 21.14 | 37.97 | 42.91 | 56.4 | 253300 | 13.49 | 19.98 | 34.22 |
| 20.01 | 9.43 | 20.53 | 36.88 | 42.96 | 56.56 | 250500 | 13.6 | 20.08 | 34.22 |
| 20.21 | 9.43 | 20.53 | 36.88 | 43.09 | 56.86 | 253700 | 13.78 | 20.17 | 34.22 |
| 19.9 | 9.43 | 20.53 | 36.88 | 43.21 | 57.06 | 257600 | 13.86 | 19.88 | 34.22 |
| 19.39 | 9.3 | 19.92 | 35.78 | 43.32 | 57.16 | 247300 | 13.84 | 19.36 | 34.22 |
| 19.36 | 9.17 | 19.31 | 34.69 | 43.39 | 57.33 | 238900 | 13.94 | 19.33 | 34.22 |
| 19.49 | 9.17 | 19.31 | 34.69 | 43.47 | 57.61 | 244700 | 14.13 | 19.49 | 34.22 |
| 18.99 | 9.21 | 19.51 | 35.05 | 43.54 | 57.82 | 244700 | 14.28 | 18.96 | 34.22 |
| 18.77 | 8.95 | 18.29 | 32.86 | 43.56 | 57.88 | 237500 | 14.32 | 18.74 | 34.22 |

on thirty-second intervals and is formatted after 24 hours into a comma separated value file for uploading as shown in the example of Table 1. The data was accessed through the secure webpage and uploaded locally to analyze how the operation modes affected cooling output. Initially the coils operated in standard ePIV mode, acquiring data during the months with the highest cooling

demand. At MIT, the output in IP units is converted to SI units for the purpose of model calibration and analysis. The variables introduced in Section 4.3 were the only ones used for calibration purposes although other variables such as DDC setpoint and valve feedback position are also provided.

## 5.3 – Data Analysis Strategies

Early on in the research it proved useful to plot power vs. flow (Figure 18) for various days to have a better understanding of the basic characteristics of the coil as well as determine a day in

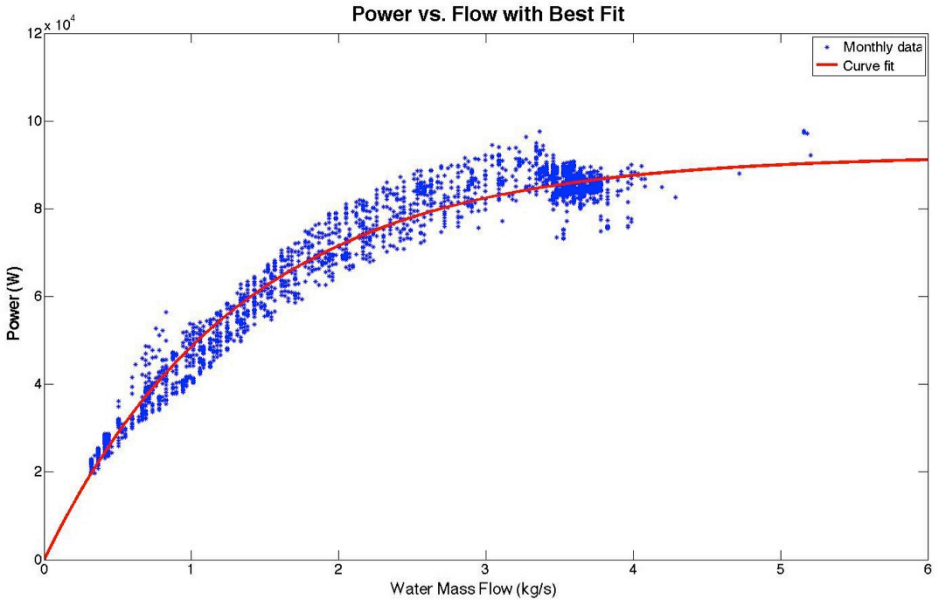


**Figure 18 - Power vs. flow curves**

which the coil was in complete saturation. Coil saturation is the point at which the rate of change of power to flow is some minimum value. It is essentially the point at which a significant increase in water flow rate does not yield a significant increase in cooling power. Compare in Figure 18 a rate of change from 0 to 1 kg/s with a rate of change from 3 to 4 kg/s. It is clear from the dense concentration of data points between 3 and 4 kg/s that the coil has reached its maximum cooling capacity. The exponential nature of the data set can be described by the following equation:

$$\dot{Q}_{cooling} = k_1\left(1 - e^{-k_2 \dot{m}_L}\right) \tag{55}$$

where $k_1$ and $k_2$ are coefficients and $\dot{m}_L$ is the mass flow of the water. As $\dot{m}_L$ approaches infinity the decaying exponential term goes to zero, leaving only $k_1$, which can be thought of as the max cooling capacity of the coil.

When looking at Figure 18, it is clear that the amount of cooling power can vary due to changing input parameters such as supply water temperature (SWT), mixed air temperature (MAT), humidity and air flow rate. If these parameters were to remain constant then the distribution of data would look similar to the red curve fit in Figure 18. This simple observation led to the development of the computer model to simulate how cooling power, and thus delta-T, is affected by changing input parameters. This combination of computer simulation and experimental data analysis gives unique perspective to a complicated problem.

# 6 Model Calibration

## 6.1 – Calibration Procedure

After analyzing the data from the various air-handling units at both MIT and CU Boulder, it was determined to use AHU-6 and AHU-1 respectively for the purpose of model calibration. Both coils serve larger zones and are easier to access then the other coils, so specific coil dimensions were easier to acquire, although it should be noted that a third party collected the dimensions and parameters of the coil. Coil height and width, tube width, fins per meter, number of rows of coils, tubes per row and number of circuits were all estimated by visual inspection rather then by using manufacturer data. Because of this visual inspection it is assumed that there will be some uncertainty in these parameters. The material properties listed in Section 4.5 were assumed to be similar to both coils and were taken from Cengel and Boles (2008). Properties of the air and water at local atmospheric conditions were also entered along with the other properties as seen in Figure 6. Since data was collected earlier at MIT it was determined to calibrate the model to data acquired on August 6$^{th}$, the day with the highest cooling demand and highest outdoor air humidity. Data collected on October 4$^{th}$ at CU Boulder was used to calibrate an additional model to further validate the model in a dry-coil situation.

Basic dimensions of both coils and material properties are well known and are taken to be valid assumptions. The parameters that were difficult to document were the coil face velocity of the entering air, number of fins per meter, tubes per row, and number of rows of tubes. The model does not account for fin pitch directly but does account for the parameter indirectly by estimating the ratio of the minimum flow area inside the core of the coil to the area of the face of the coil. The minimum flow area within the core of the coil is determined by the density of fins and whether the fins are flat plate or wavy. This value is undetermined and therefore should be considered as a variable to be changed for the purpose of tuning the model to both air handling units. According to McQuiston et al. (2005) the heat transfer rate of the plate-fin-tube coil decreases for each successive row of the coil. An average heat transfer rate is calculated by using the j-factor described in Equation 9. Because of this uncertainty, the parameter that directly affects the heat transfer rate in Equation 9 is the mass flux of the air defined by:

$$\phi_{air} = \frac{\dot{m}_{air}(1+g_o)}{\frac{A_c}{A_f}A_f} \tag{56}$$

where $A_f$ is the coil face area, $g_o$ is the humidity ratio and $\frac{A_c}{A_f}$ is the ratio of the minimum flow area in the core to the face area (McQuiston, Parker and Spitler 2005). The mass flow rate of the air is defined as

$$\dot{m}_{air} = \phi_f A_f = \phi_c A_c \tag{57}$$

The flux of air through each coil can then be determined by solving Equation 56, using the minimum flow area ratio in the denominator. Once the basic dimensions and parameters of each coil were entered a simulation was run comparing the output with the actual data. The following table displays the variables that were changed to calibrate the model.

**Table 2 - Tuned parameters for both cooling coils**

| | Tuned Parameters | | | | | |
|---|---|---|---|---|---|---|
| | Coil | Fins per meter | Rows of tubes | Tubes per row | Number of circuits | Face velocity ratio |
| Initial Values | MIT | 350 | 6 | 34 | 4 | 0.62 |
| | CU Boulder | 360 | 4 | 30 | 4 | 0.62 |
| Tuned Values | MIT | 380 | 8 | 36 | 4 | 0.72 |
| | CU Boulder | 400 | 8 | 34 | 4 | 0.75 |

Supply air temperature, supply air enthalpy, return water temperature and total waterside and airside heat transfer rates of the simulation were compared with the measured data from the sensors installed in both air handling units

## 6.2 – MIT Calibration Results

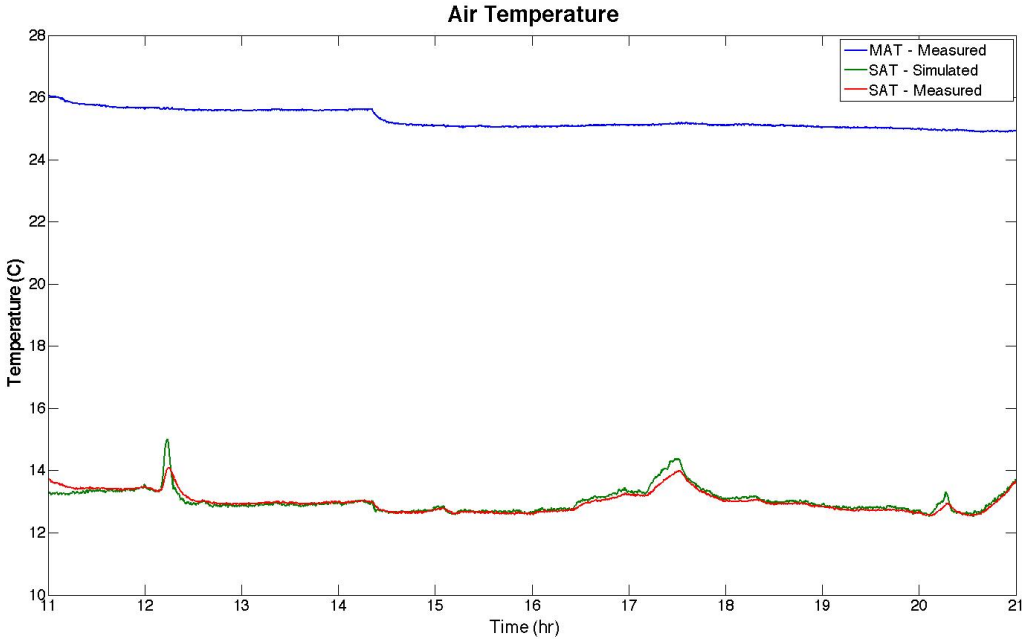


**Figure 19 - AHU-6 air temperature calibration results**

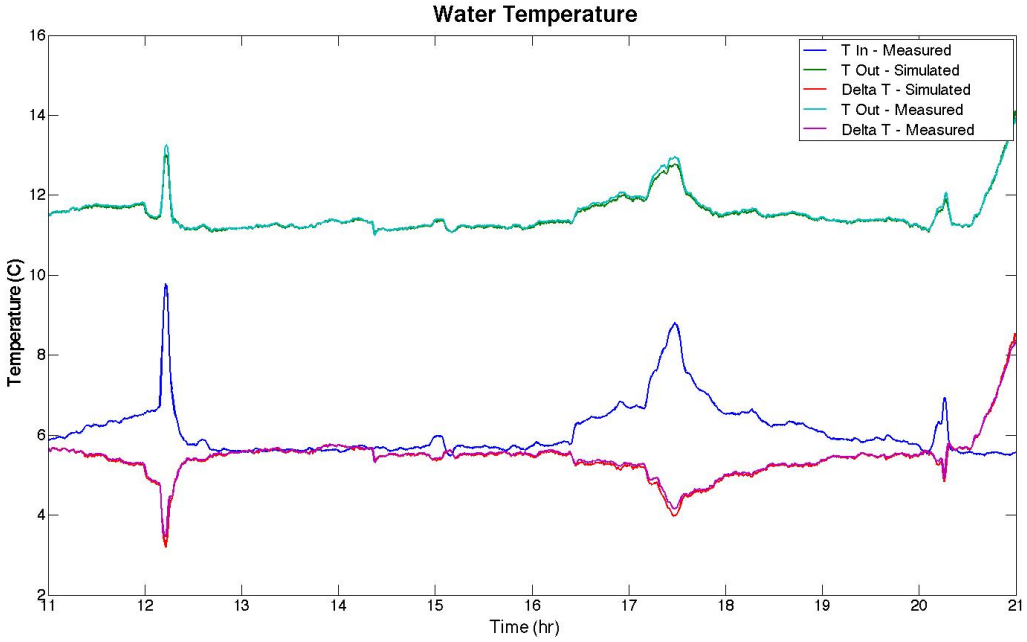


**Figure 20 - AHU-6 water temperature calibration results**

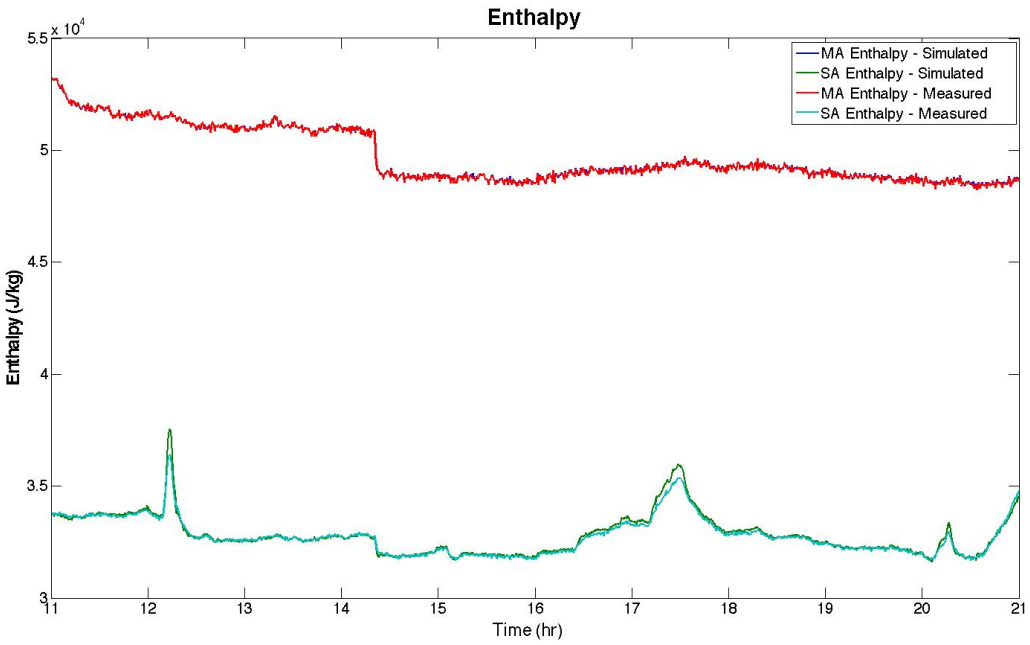


**Figure 21 - AHU-6 enthalpy calibration results**

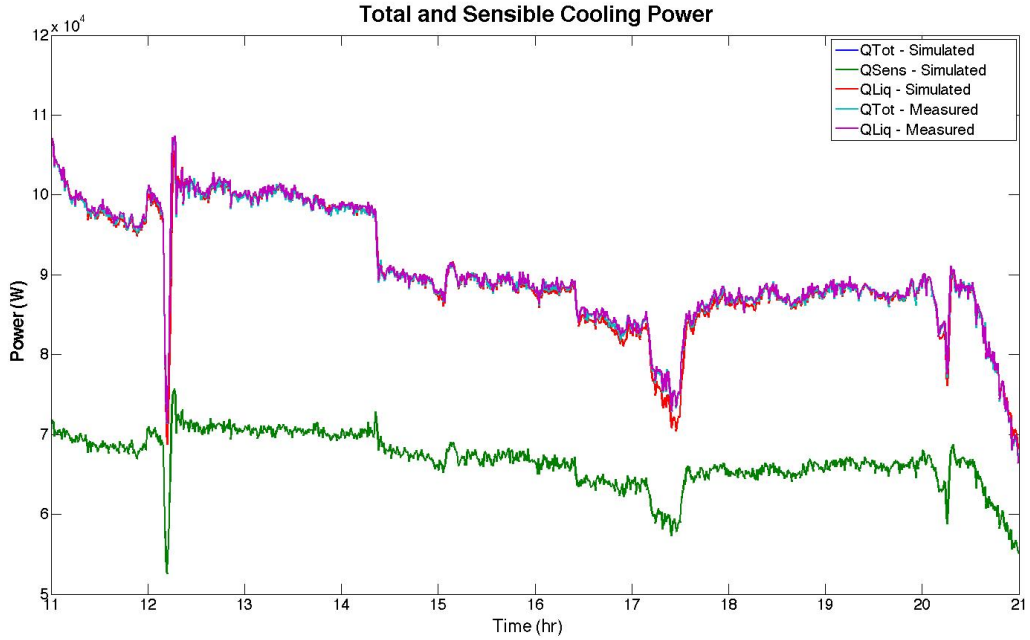


**Figure 22 - AHU-6 cooling power calibration results**

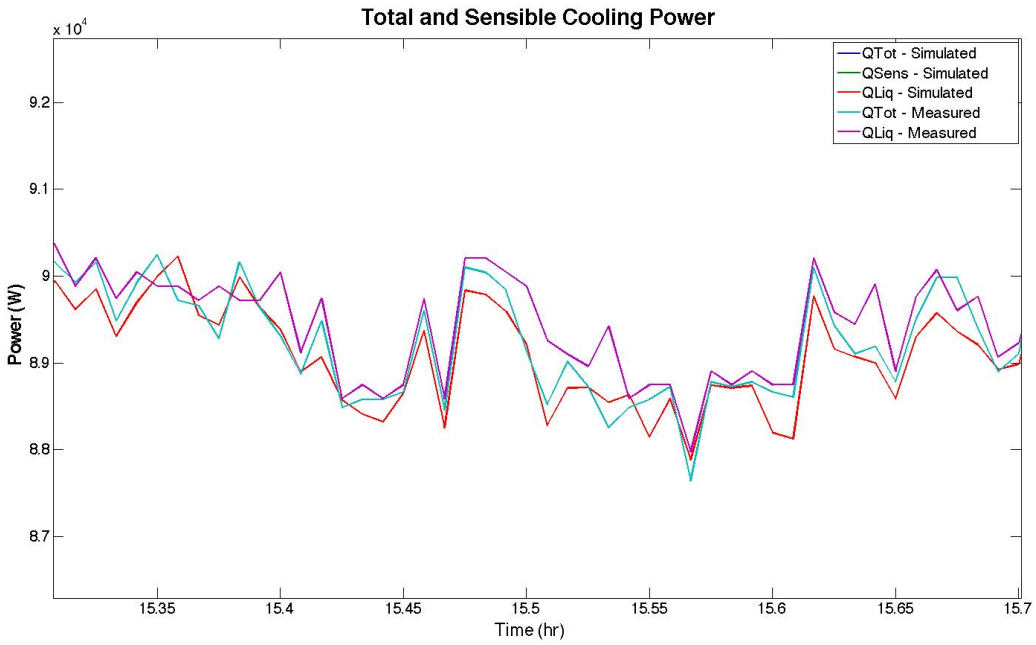


**Figure 23 - AHU-6 energy balance validation**

The calibration results displayed in the previous figures are for operating hours only. The system is shut down during the night and therefore allows the temperature to float. As mentioned previously MIT experiences conditions in which dehumidification within the coil occurs. This results in mostly latent heat transfer. Figure 23 validates the energy balance of both the simulation and the measured data. Upon closer inspection the simulation total and waterside heat transfer rates are exactly the same. When looking at the measured data there is some variation between these values. This is due to the slight error in the airside sensors as seen by the variation between the light blue and red curves.

## 6.3 – CU Boulder Calibration Results

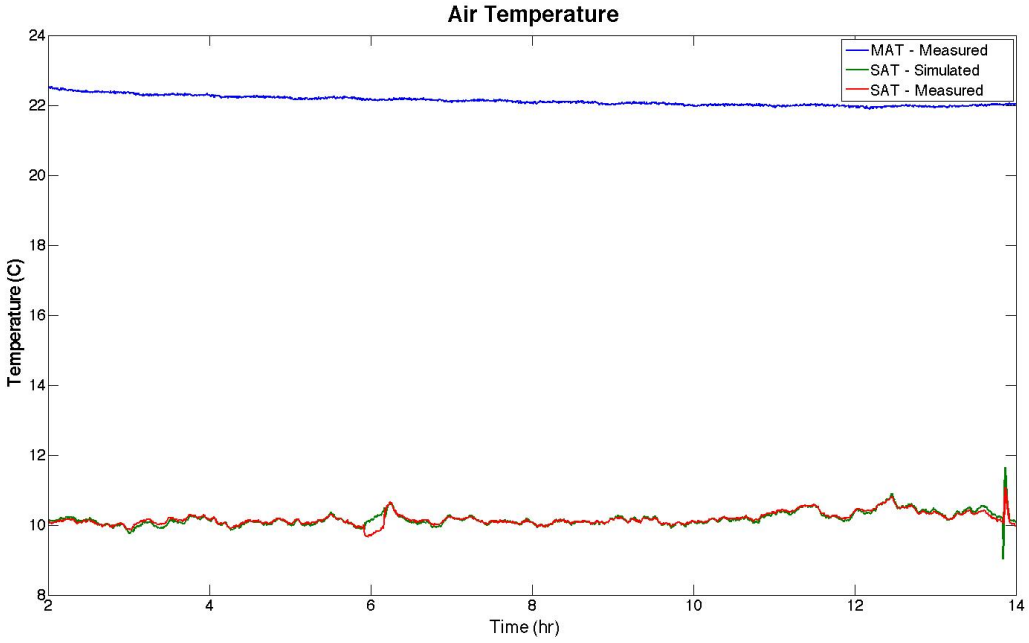


**Figure 24 - AHU-1 air temperature calibration results**

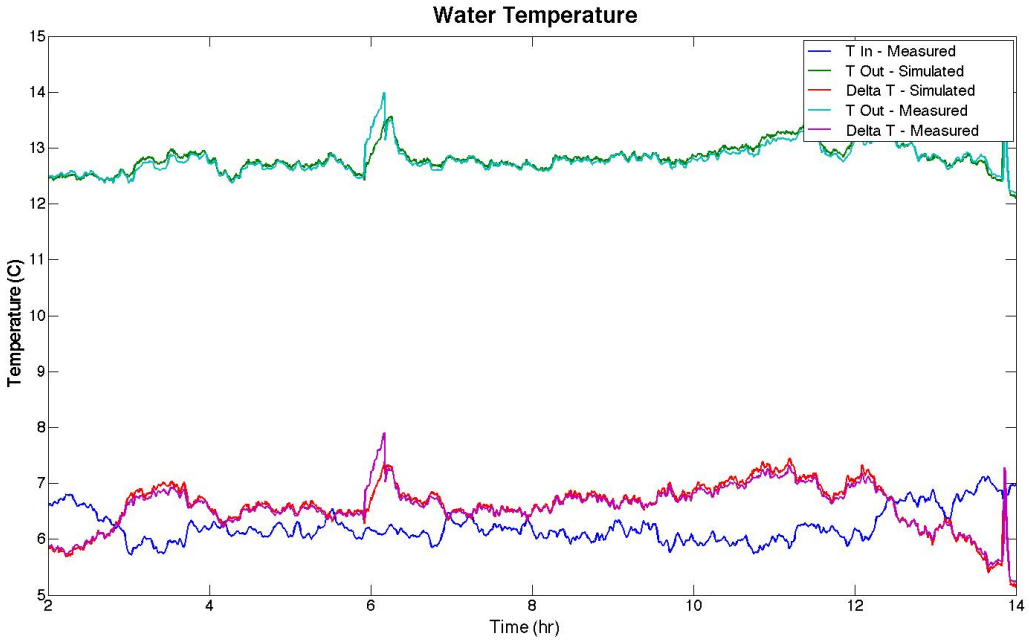


**Figure 25 - AHU-1 water temperature calibration results**

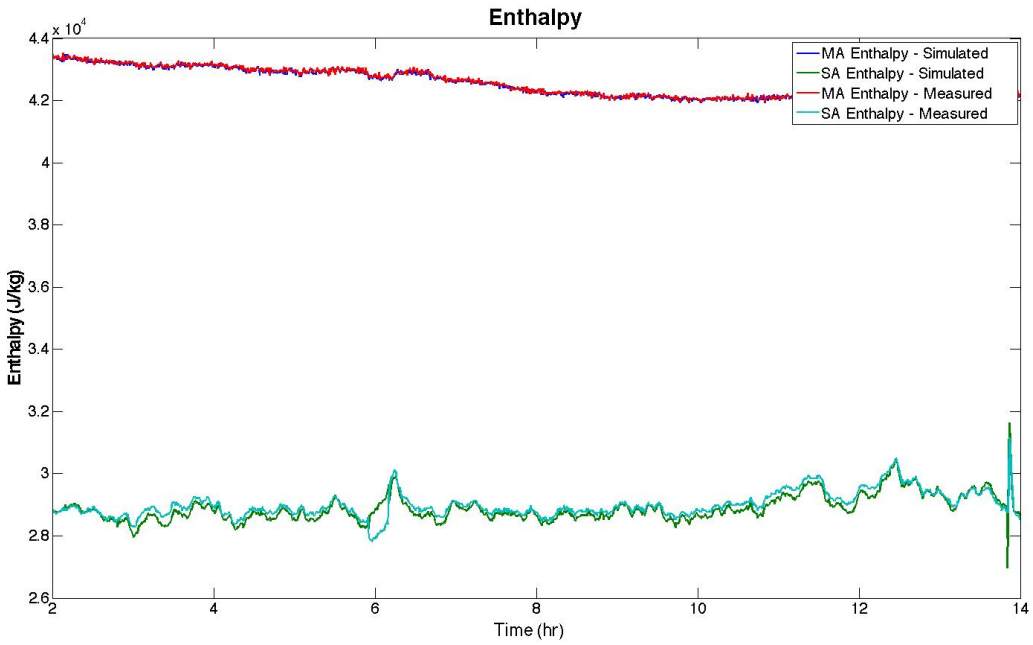


**Figure 26 - AHU-1 enthalpy calibration results**

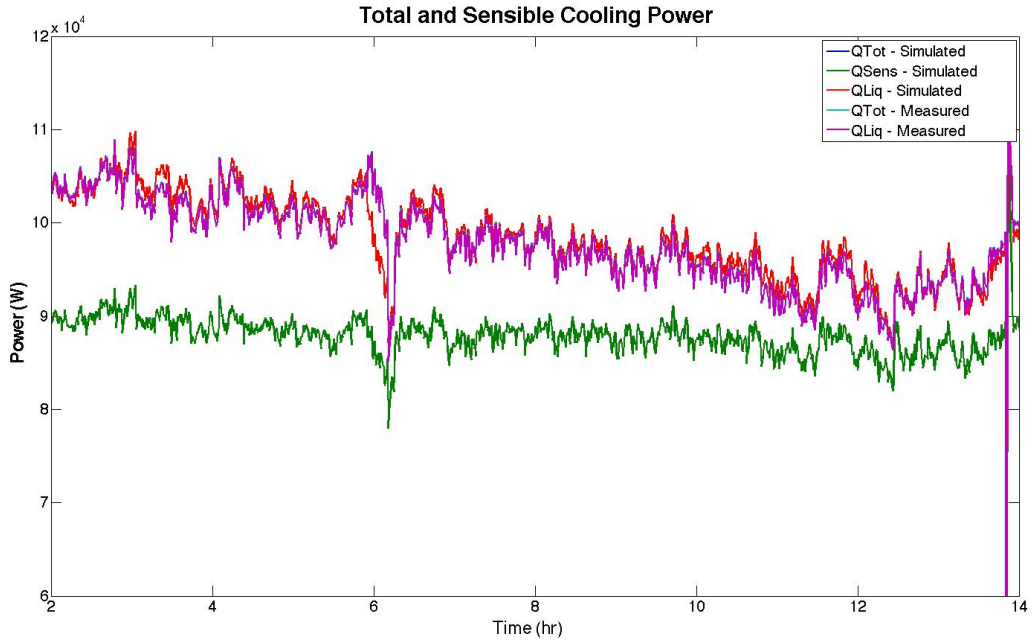


**Figure 27 - AHU-1 cooling power calibration results**

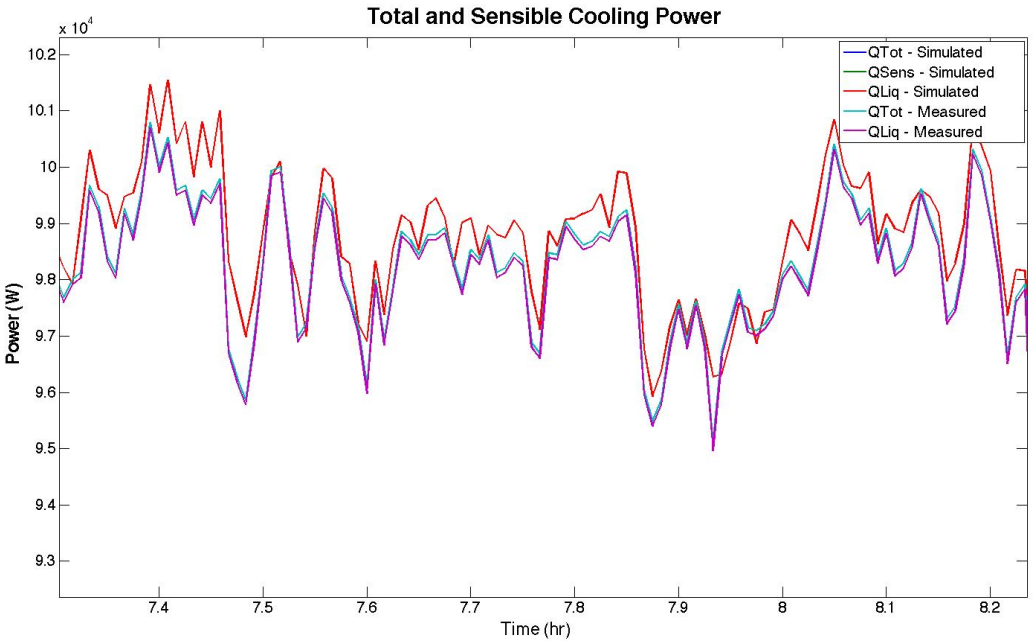


**Figure 28 - AHU-1 energy balance validation**

The results from CU Boulder are consistent with the results from MIT. There is however some variation between the simulation and the measured data upon closer inspection of the previous plots.

## 6.4 – Root Mean Squared Error Analysis

The variation between the simulation and measured data is further investigated by performing error analysis on the data set using the root-mean-square error method. The RMSE is a way to measure of the average deviation of the simulation from the actual measured data. At each time step the difference between the simulated data point and the measured data point is calculated then squared. The square root of the average of these values is then calculated to produce an average measure of deviation. The difference between the simulated values and the measured values and is defined as follows:

$$RMSE(x_1, x_2) = \sqrt{\frac{\sum_{i=1}^{n}(x_{1,i}-x_{2,i})^2}{n}} \tag{58}$$

where $x_{1,i}$ is the measured value, $x_{2,i}$ is the simulated value and $n$ is the number of values in the data set.

Error analysis was completed for the output variables in Figure 19 through Figure 28 and are displayed in the following table:

**Table 3 - Error analysis results**

| | Supply Air Temperature | Mixed Air Enthalpy | Supply Air Enthalpy | Return Water Temperature | Delta-T | Q Total | Q Liquid |
|---|---|---|---|---|---|---|---|
| MIT RMSE | ± 0.75 ˚C | ± 25 J/kg | ± 150 J/kg | ± 0.10 ˚C | ± 0.15 ˚C | ± 550 W | ± 916 W |
| | | | | | | | |
| CU RMSE | ± 0.72 ˚C | ± 80 J/kg | ± 232 J/kg | ± 0.15 ˚C | ± 0.132 ˚C | ± 881 W | ± 1012 W |

Temperature sensors typically have an acceptable error of plus or minus 0.3 degrees Celsius on both the water and airside measurements while enthalpy sensors are accurate to plus or minus 2 percent (ASHRAE 2009).

## 6.5 – Kline-McClintock Uncertainty Analysis

In order to better understand how well the simulation compared with the measured data, it was necessary to investigate how the error within each sensor propagates through to the experimental calculation of total cooling power of the coil. The total cooling power derived in Equation 1 is a function of water mass flow, and the temperature difference between supply and return water. The valves are equipped with an inline magnetic flow meter upstream of the valve. The accuracy of the flow meter is measured to be 0.5 % of the flow of the water. The temperature sensors used in the experiment are coupled and calibrated together. The error associated with a coupled temperature sensor is typically lower then the accumulated error of individual sensors. The absolute error in the temperature sensors is therefore a function of delta-T rather then the individual SWT and RWT readings. The error of the sensor used is given by the following equation:

$$Absolute\ Error = \pm (0.005 \times \Delta T + 0.13)\ \mathrm{K} \tag{60}$$

The error associated with the sensors therefore affects the calculated total cooling power. The logic within the actuator uses temperature and flow readings to calculate the total cooling power for the coil at each time step using Equation 1. A Kline-McClintock uncertainty analysis was performed on the measured data in which upper and lower bounds for the total cooling power (W) are calculated using the following formula:

$$w_Q = \sqrt{\left(\frac{\partial Q}{\partial \dot{m}_L} w_{\dot{m}_L}\right)^2 + \left(\frac{\partial Q}{\partial \Delta T} w_{T_{\Delta T}}\right)^2} \tag{61}$$

Partial derivatives with respect to water mass flow, and the waterside temperature difference are calculated as follows:

$$\frac{\partial Q}{\partial \dot{m}_L} = C_P \, \Delta T \tag{62}$$

$$\frac{\partial Q}{\partial \Delta T} = \dot{m}_L C_P \tag{63}$$

The error associated with the flow sensor, and temperature sensors can be represented by the following equations:

$$w_{\dot{m}_L} = \dot{m}_L * 0.005 \tag{64}$$

$$w_{T_{\Delta T}} = (0.005 \times \Delta T + 0.13) \tag{65}$$

Equation 61 returns the uncertainty in the measured calculation of the total cooling power at each time step. The simulated results can then be compared against the upper and lower bounds of the uncertainty analysis. The uncertainty analysis was conducted for both MIT and CU Boulder at every time step although results were only plotted on hourly time intervals as seen in Figure 29 and Figure 30. When looking at the results in Figure 29 and Figure 30 it is clear that the error associated with the sensors vary. The simulated values fall between the upper and lower bounds of the error analysis it is valid to assume that the simulation produces accurate results. Because of the error in the sensors the measured results have this uncertainty, and since the simulation falls within this uncertainty it is concluded that the simulation is acceptable.

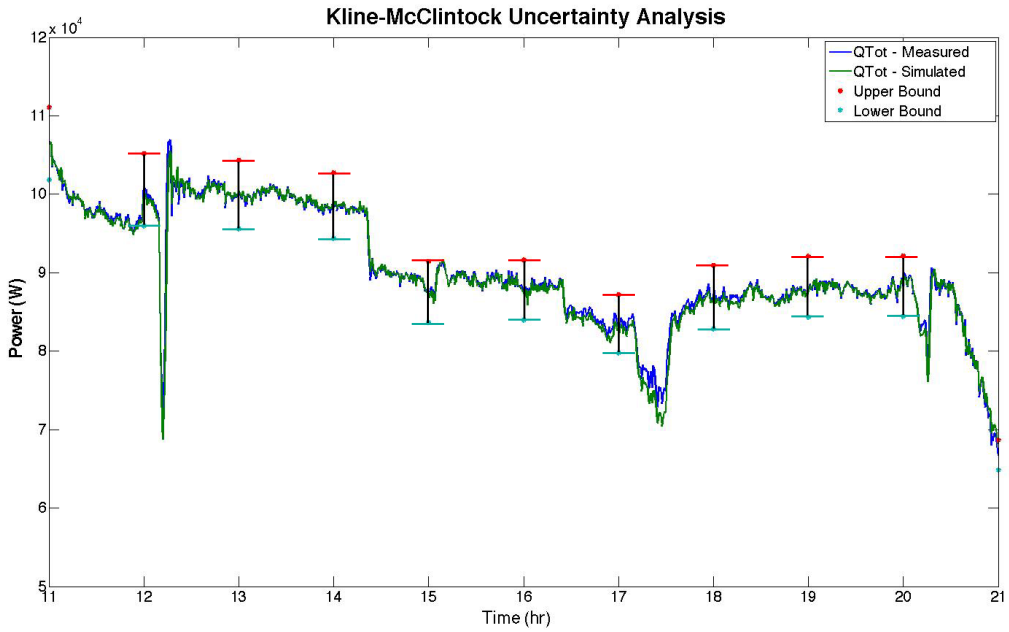


**Figure 29 – Kline-McClintock uncertainty analysis for MITs AHU-6**

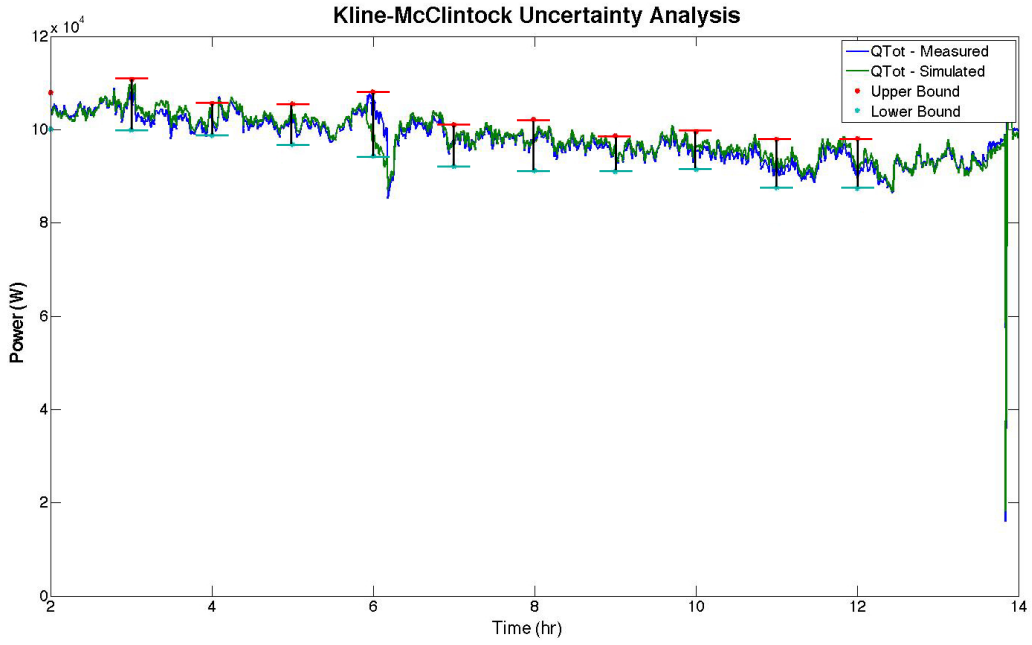


**Figure 30 - Kline-McClintock uncertainty analysis for CUs AHU-1**

# 7 Results and Recommendations

Using the calibrated model, various simulations were performed to investigate how heat transfer rates vary with the changing input parameters mentioned previously. Heat transfer rates directly affect the waterside delta-T so it is important to understand how a delta-T for a particular coil is affected by changing input parameters. This particular investigation in delta-T was necessary for understanding the consequences of entering a particular delta-T setpoint in the control logic of the

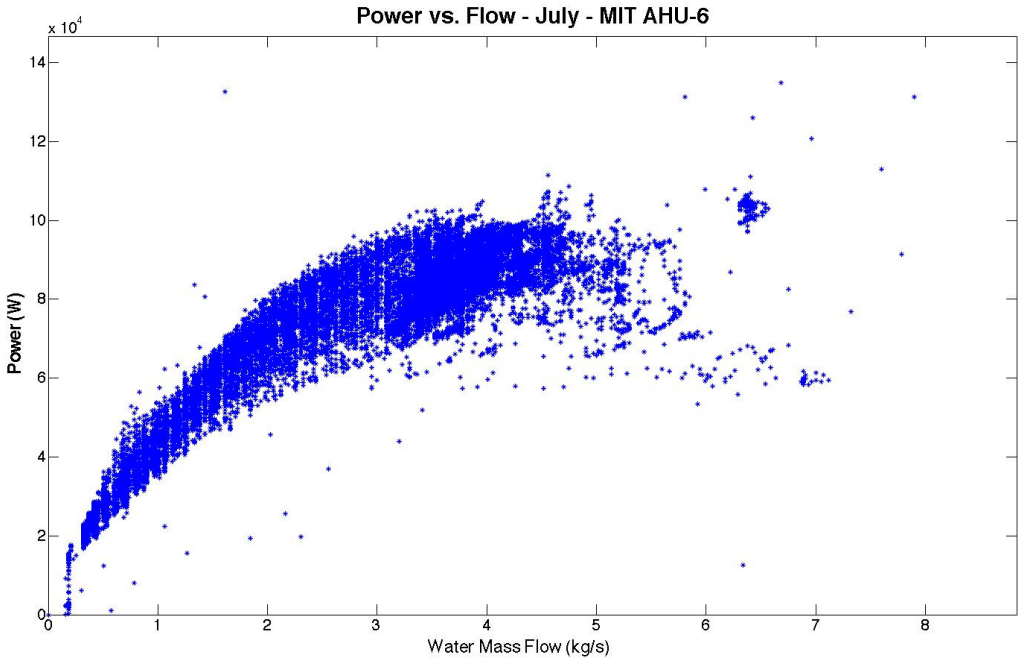


**Figure 31 - Measured data for obtained from AHU-6**

actuator used in the case study. In order to understand how a single variable affects the cooling output, and therefore the waterside temperature difference, it was necessary to perform the simulations in a way that would isolate the variable in question. When looking at the plot of power vs. flow in Figure 31, the distribution of data indicates that the cooling output is affected by multiple factors. The cooling power of AHU-6 ranges from 60,000 to 100,000 Watts, which is considerable when trying to maintain a desired cooling power to the zone. MITs facilities maintenance operates AHU-6 with a constant SWT but after analyzing the data it was clear that it deviates considerably. AHU-6 experiences SWT fluctuations up to 4 Kelvin and mixed air flow rate fluctuations up to 17 percent. The fluctuations in SWT can be attributed to an overloaded central plant in which the central chillers cannot meet demand, thus allowing the SWT to float. It was necessary to have a

better understanding of the effect a small fluctuation in a supply variable has on the overall performance of the coil.

## 7.1 – Steady State Analysis

Multiple simulations were performed in which every input variable was held constant while one control variable was allowed to change (Table 4). When looking at the SWT influence, for example, air

**Table 4 - Constant variable data**

| Constant Variables used in Simulation | | | |
|---|---|---|---|
| SWT | MAT | Air Flow Rate | Relative Humidity |
| 7 °C | 25.5 °C | 6.5 kg/s | 50 % |

mass flow rate, air temperature and humidity were all held constant. A simulation can then be run that isolates the SWT variable. A base case was established in which all variables were held constant while water mass flow rate increased from 0 to 10 kg/s (l/s) (Figure 32). The blue curve of Figure 32 represents the cooling power while the green curve is the delta-T value at a specific mass flow rate. As the water flow increases cooling power exponentially increases towards a limit, while the delta-T decreases in an inverse fashion. The curves in Figure 32 corresponds to the classical textbook power vs. flow curve and is typically what is represented in the majority of textbooks and manufacture data on cooling coils.

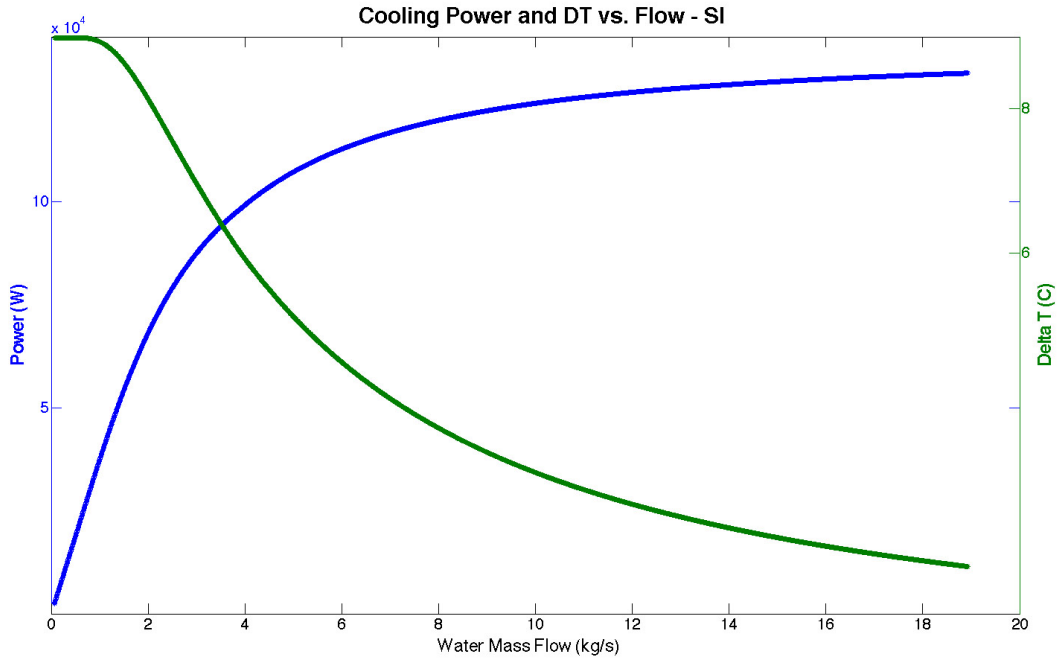


**Figure 32 - Base case simulation**

How are the shapes of the power and delta-T curves affected when supply conditions change? Let us examine what happens when the supply water temperature rises from 5 °C to 9 °C, a realistic change identified in the SWT of AHU-6. A 4-Kelvin increase in SWT limits the cooling capacity of the coil by approximately one-third. The distribution of data in Figure 31 is clearly affected by SWT

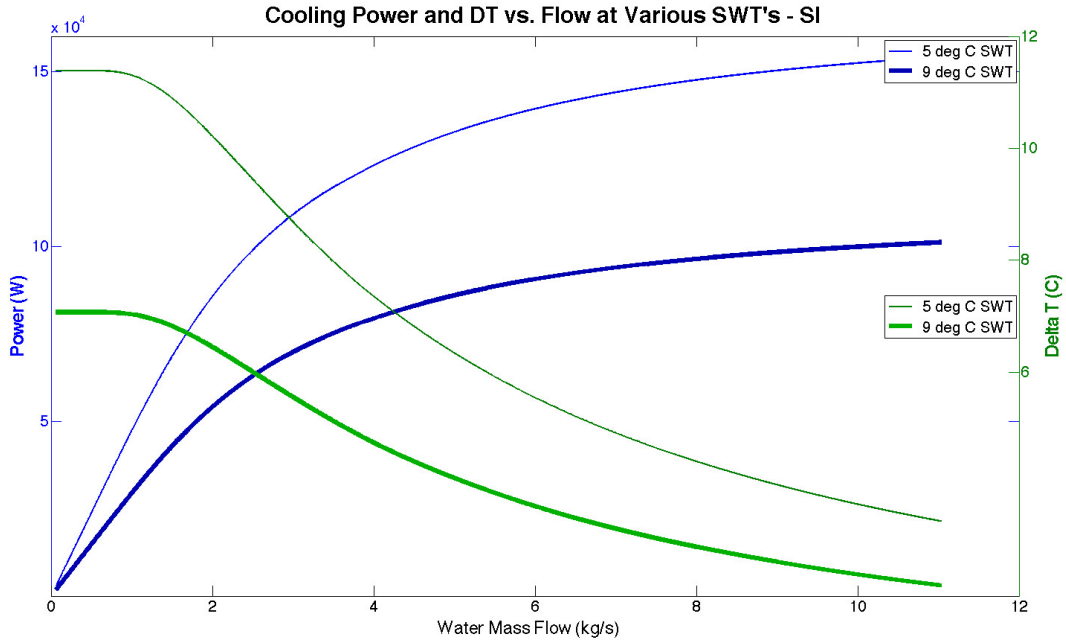


**Figure 33 - Affect of SWT fluctuation on cooling power and DT**

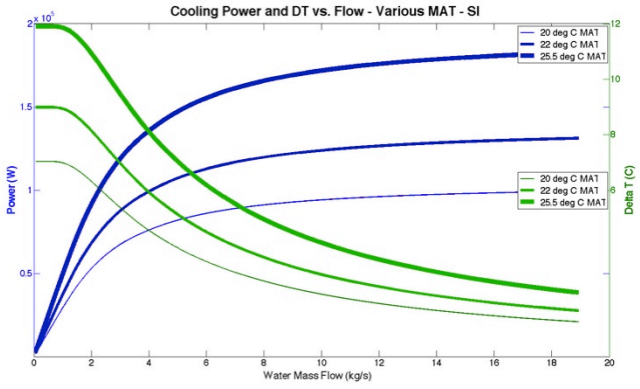


**Figure 34 - Rise in MAT**

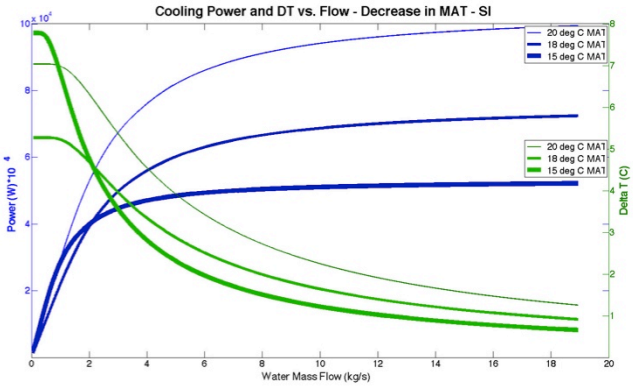


**Figure 35 - Drop in MAT**

when a comparison is made to Figure 33. A similar trend is seen in when the temperature of the mixed air is allowed to float. When the MAT is at 15 °C the dew point temperature remains below the entering water temperature indicating the coil will only have sensible heat transfer. In this case the coil reaches capacity much quicker thus going into saturation much sooner and because of the lack of mass transfer there is less heat transfer at any given flow rate. Variations in relative humidity have a similar affect on cooling capacity especially when the dew point temperature of the air is greater then the entering water temperature. At this point water vapor in the air begins to condense on the coil surface in the process described in the section on model development. The simulation, as

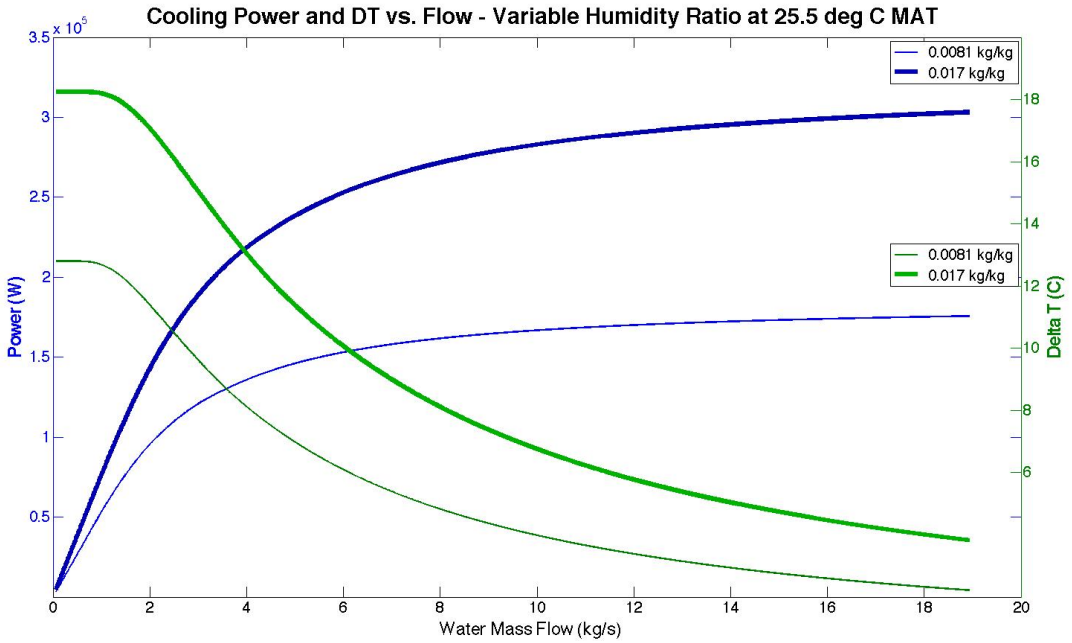


**Figure 37 - Affect of variable humidity ration on cooling power and DT**

seen in Figure 37, outputs the results in terms of humidity ratio, which is a much better measure of the amount of moisture in the air at a given temperature. The equivalent relative humidity increase would be approximately from 35% to 90%. When the amount of moisture in the air doubles the amount of total (sensible and latent) cooling power achieved increases by a factor of two.

These fluctuations seen in supply variables greatly affect the cooling output of the coil; therefore choosing the correct delta-T or flow limit for particular cooling coil is essential to maximize cooling performance of the coil in question. Typically coil manufactures recommend a design delta-T based on static supply conditions but as seen in Figure 33 to Figure 37, fluctuations in supply variables have considerable influence on both power and delta-T. It is evident then that the installed characteristics of a coil can be quite different from that of the manufacture specifications. If a

particular hydronic system is designed using a certain delta-T and the supply water temperature increases, the coil will no longer behave as it would at design levels as seen in Figure 33. This is of particular importance when designing intelligent control devices and hydronic systems. The control logic in the actuator of the valve used in AHU-6 uses two strategies to maximize cooling power of

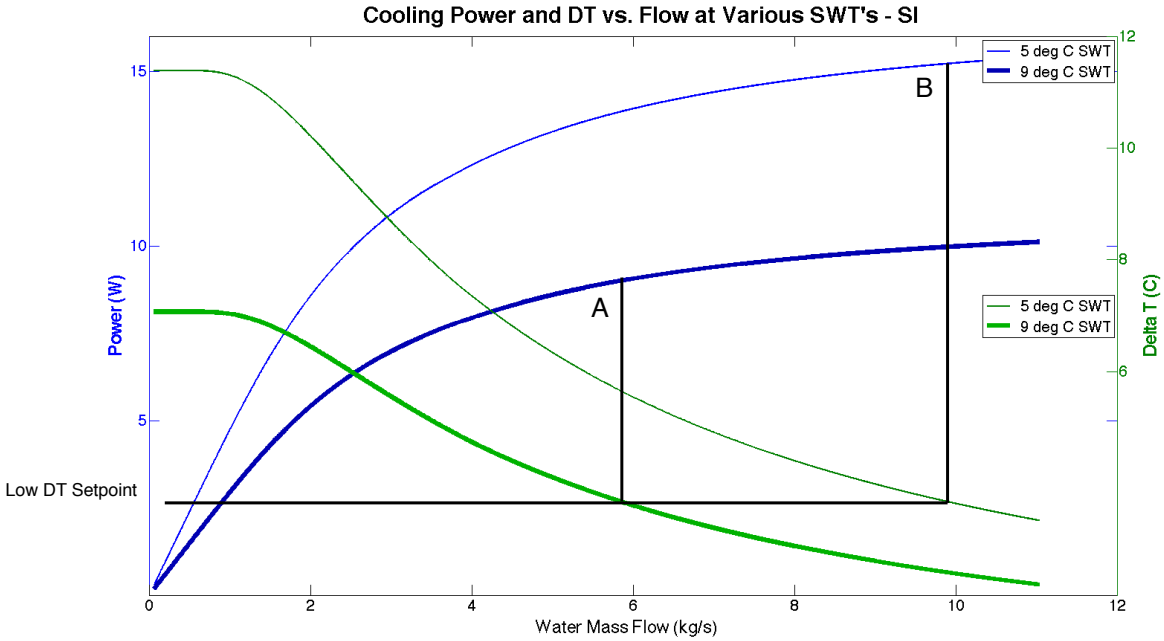


**Figure 38 - Various DT setpoint limits**

the coil. The first strategy is to maximize the delta-T across the coil directly. This is achieved by controlling flow to maintain a measured delta-T within limits of a setpoint. When the valve is initially commissioned, a delta-T setpoint for the particular coil is entered according to coil manufacturer specifications. The logic then controls to maintain water flow at or above the desired setpoint. In order to better optimize the cooling output it is necessary to define a delta-T that is not only correct for the particular coil but also correct for the particular hydronic system. This will ensure that the coil does not operate in the saturation zone, which wastes considerable pumping energy. The second strategy limits the flow for a particular coil at a flow setpoint, which also prevents the coil from operating in the saturated zone. Both delta-T and flow limiting strategies are investigated further. It is necessary to understand how both these strategies can aid the engineer in designing more efficient systems.

Let us examine the case in Figure 38. The light blue curve shows Power vs. Flow at a design SWT of 5 °C. When considering a delta-T setpoint the limiting point on the curve would be point B

at a 5 °C SWT. In this case if the SWT increases to 9 °C, cooling would be limited at point A. Similar to Figure 31 there is a large operating range of the coil when SWT fluctuates. It is clear that if a low delta-T is selected and the SWT rises there will be a significant decrease in cooling power and the coil still remains in saturation. This is significant when designing hydronic systems and must be considered to better optimize the cooling performance of the coil. For example, if the optimal

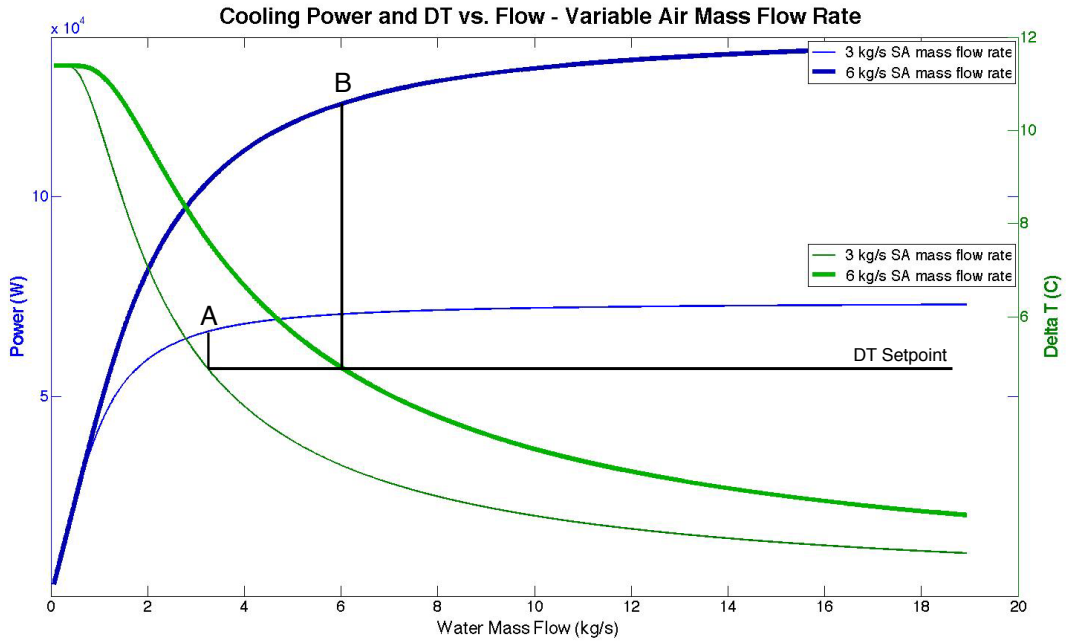


**Figure 39 - Affect of variable airflow rate on cooling power and DT**

delta-T were selected for a particular coil at various SWTs cooling output could be optimized. Now let us consider a flow limiting strategy for the case in Figure 38. If a flow limit was imposed on the coil at 6 kg/s and the SWT increased from 5 to 9 °C cooling output would decrease by 33 % while pumping power remains constant.

Finally, a similar analysis was completed for consideration when using variable volume systems. VAVs are quickly becoming the retrofit of choice for many HVAC systems due to the fact that they save considerable fan energy. Based on Equation 1 it would be valid to see a proportional increase in cooling power to an increase in airflow rate. In Figure 39 an increase in mass flow rate from 3 to 6 kg/s sees a proportional increase in power from 75,000 to 150,000 Watts. Let us examine the influence a particular delta-T setpoint has on a VAV system. When looking at Figure 39, if a delta-T is selected and the airflow doubles the power and delta-T curves scale proportionally with no affect on the operating point of the coil. The points A and B remain directly before the saturation point of the coil regardless of the change in airflow.

From all of the previous simulations it is evident that the coil reaches a maximum operating capacity for each set of input variables. SWT variation seems to have the greatest affect on the maximum cooling output and ultimately the delta-T across the coil. VAV systems also are not as sensitive to delta-T setpoints imposed. It is important to be able to identify the maximum operating capacity of a given coil during actual operation for the purpose of limiting the coil from operating in the saturated zone and to choose a delta-T or flow limit that will be accurate for the installed system and for a various supply conditions. Based on the simulation in Figure 33 it is evident that each coil will effectively have a maximum cooling capacity for a particular SWT. Each range of SWTs will yield its own unique coil curve and thus have a unique saturation point. The challenge arises in determining the proper saturation point and thus a delta-T value or flow limit that optimizes the output of the coil in question. By understanding the affect of a particular delta-T or flow setpoint engineers will be able to maximize the performance of the designed systems resulting in increased comfort and decreased pumping power. Section 7.3 of this research focuses on developing a tool which is used to aid in the commissioning process of the new valve, eliminating any error in choosing the wrong delta-T or flow limit.

## 7.2 – Measured Data Results

Based on the results from the simulation it was necessary to develop a better understanding of how the actual coil in AHU-6 behaves as supply conditions change, particularly SWT. Each month of data was analyzed in order to understand what happens in the actual system. Cooling power and delta-T values for discrete SWTs intervals was binned and plotted against the water mass flow rate for the months of July, August and September, the months with the greatest cooling demand.

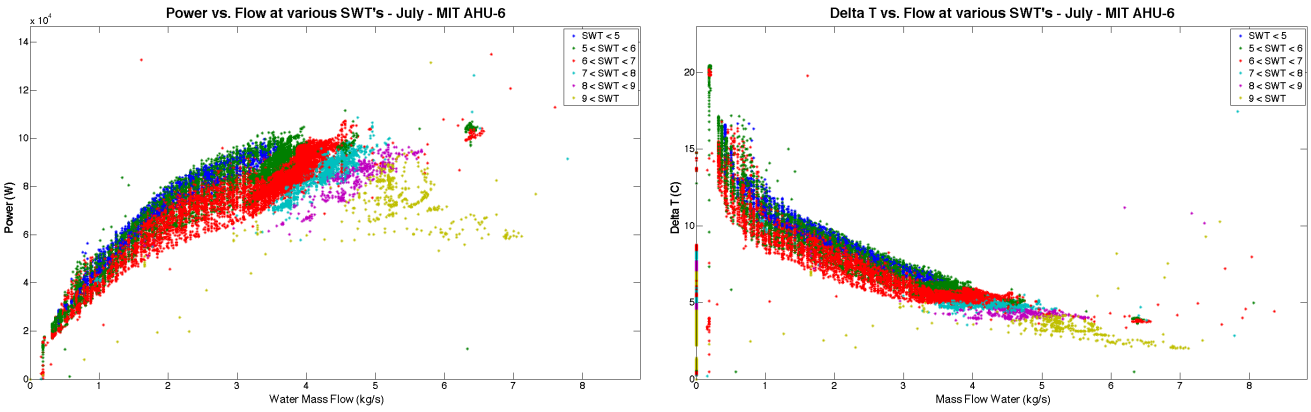


**Figure 40 - Cooling power and DT during July at various SWT intervals**

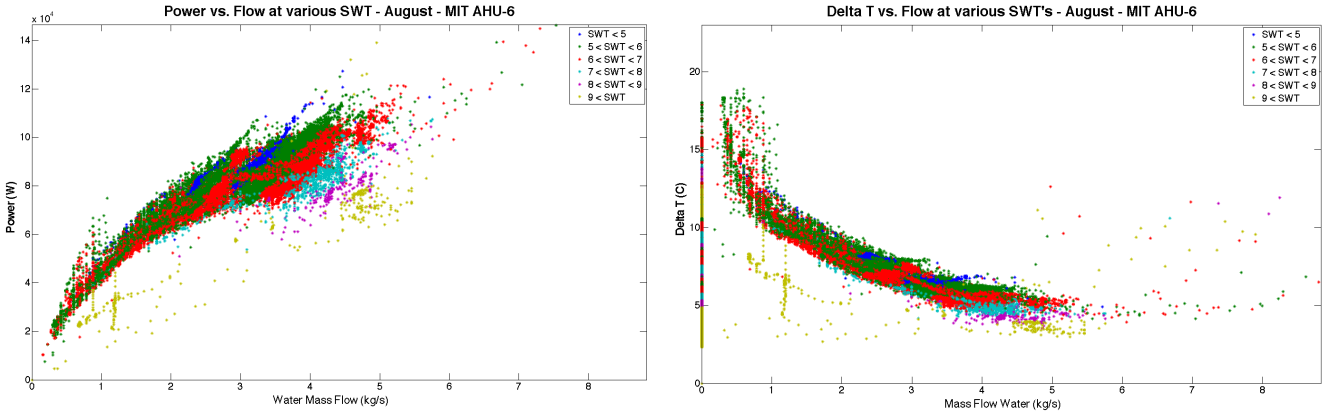


**Figure 41 - Cooling power and DT during August at various SWT intervals**

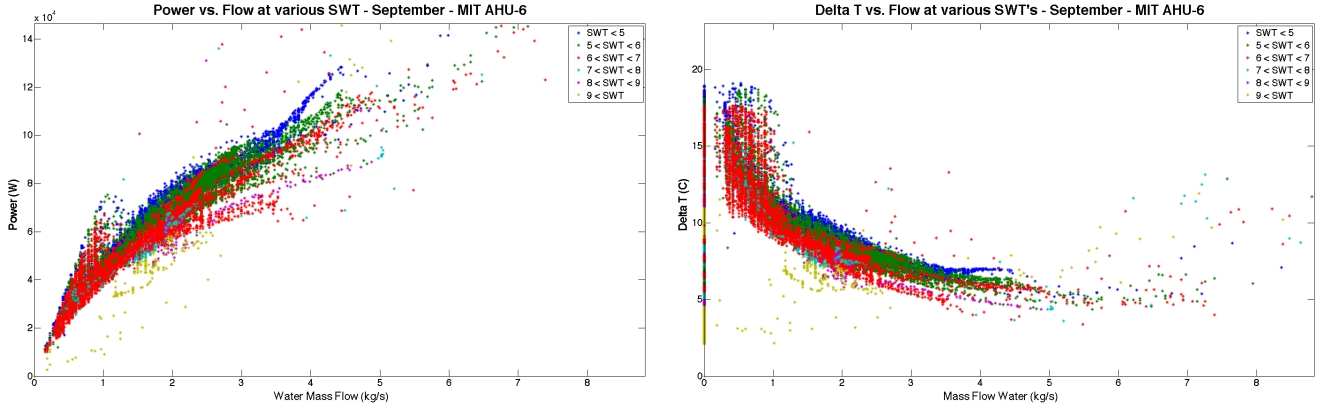


**Figure 42 - Cooling power and DT during September at various SWT intervals**

By looking at Figure 40 through Figure 42, it is apparent that the SWT increase does have a significant influence on the cooling output of the coil. Let us examine Figure 40 a bit closer. When the SWT is less then 5 °C (blue) the coil reaches a capacity of 100,000 Watts. As the SWT increases between 6 °C and 7 °C, the concentration of red data points increases dramatically. When the SWT increases even further the output of the coil decreases. Based on Equation 55

$$\dot{Q}_{cooling} = k_1\left(1 - e^{-k_2 \dot{m}_L}\right)$$

it holds that for a particular coil there will be an exponential increase in power towards some maximum value of $k_1$. This maximum value is heavily influenced by the SWT, which is why the trend of the data in Figure 40 decreases. The saturation point of the coil in Figure 40 is the point at which there is a high concentration of data points as seen with the red data points at a water flow of

4.7 l/s. This is more difficult to distinguish in Figure 42 because the coil is operating at part-load. While the SWT does have an influence on the cooling power the coil does not seem to be operating at full capacity or in the case of Figure 40, past the most efficient capacity.

It will be easier to visualize the trend of the data in Figure 40 by fitting a curve to each SWT data set as seen in Figure 43. Using the built in Levenberg-Marquardt algorithm in Matlab the curve described in Equation 55 was fit to each SWT data set. The L-M algorithm provides a numerical

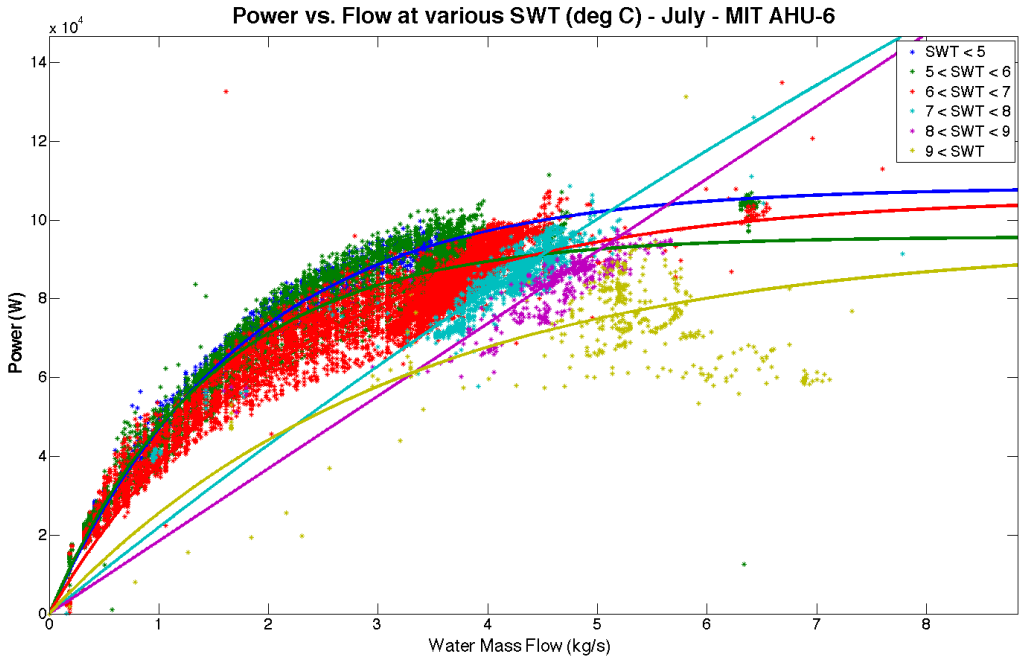


**Figure 43 - Curve fit for each SWT interval using L-M algorithm**

solution to the problem of minimizing the difference between the measured value of power and the predicted value described in Equation 55. The solution is found by iteratively minimizing the following function:

$$f(\dot{m}, k_1, k_2) = \sum_{i=1}^{m} \left[\dot{Q}_i - \left(k_1\left(1 - e^{-k_2 \dot{m}_i}\right)\right)\right]^2 \tag{59}$$

Since the L-M algorithm is an iterative process it requires an initial condition to start. The initial conditions for $k_1$ and $k_2$, for the purpose of this data set is 100,000 and 0.03 respectively. Care should be taken when choosing the initial conditions of $k_1$ and $k_2$ as it affects convergence within the algorithm. It should be noted that the distribution of data greatly affects the confidence in the fit

and the guarantee of convergence. This can be seen in Figure 43 by looking at the light blue and purple curves. The curve fit appears to be linear because of the lack of convergence of the coefficients. When the SWT is above 7 °C the coil is operating in saturation. The data at this point is concentrated in a manner that is not described by the exponential function of Equation 55. The algorithm therefore cannot accurately fit a curve to that set of data. As water temperature increases, one would expect an exponentially increase towards lower and lower final values as seen with the blue, red and green curves. This simple example illustrates the point that using a curve to fit the data is only as good as the data that is used to fit the curve.

## 7.3 – Excel Tool Development

Based on the previous analysis it was necessary to develop a tool that would assist building engineers in setting a proper delta-T or flow limit for the actuator logic. By providing the customer

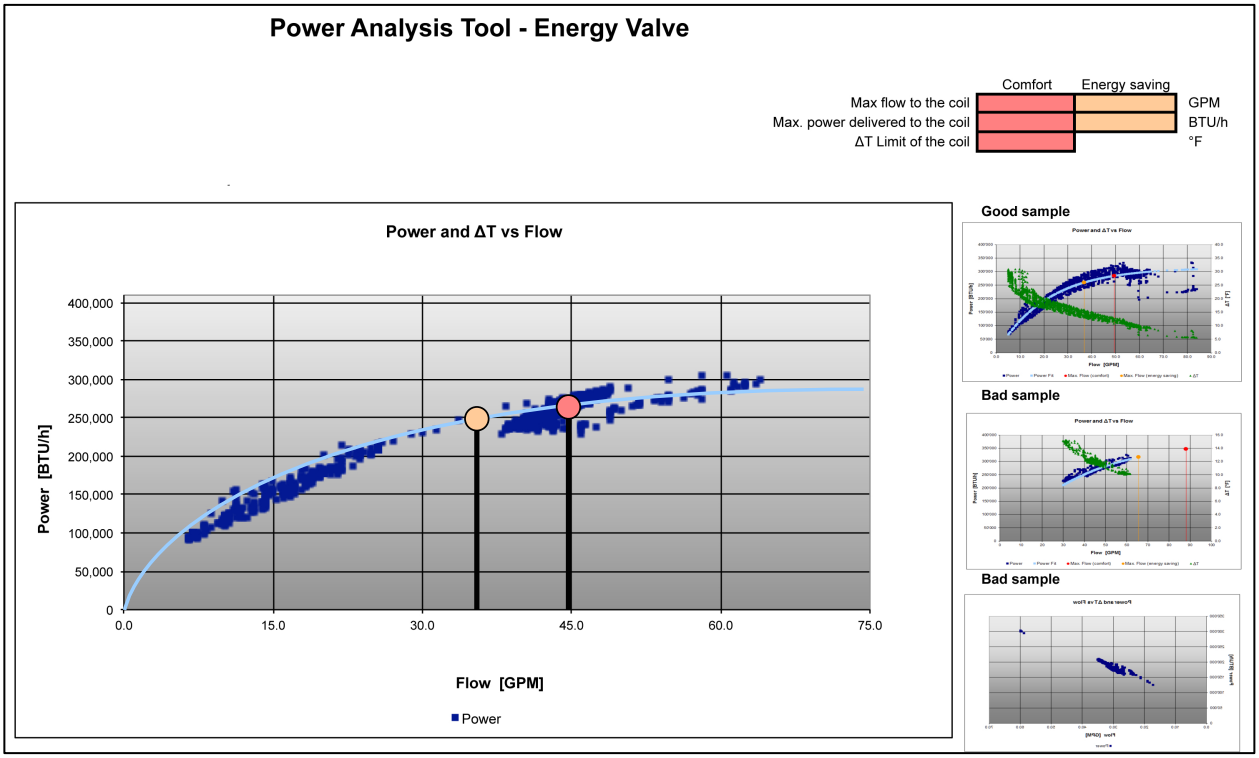


**Figure 44 - Excel tool output window**

with a tool to set a delta-T or flow limit, the error associated with choosing an incorrect value can be reduced. For instance, the coil manufacturer may recommend setting the delta-T of 10°C, which is usually experimentally based on a constant SWT. The installed characteristic of the coil can very greatly from that of the experimental coil, thus causing the manufactured recommended delta-T

value to be less effective at limiting the coil from operating in the saturated zone. If the SWT tends to float a slightly lower delta-T could possible be more effective, though a visual aid would help confirm the correct setpoint during the commissioning phase of the new valves.

The tool, which is developed in Excel, uses a procedure to automatically identify a correct delta-T setpoint and flow limit for an individual coil. Initially the intelligent valve will operate as a standard ePIV while the actuator gathers data over a period of 3 weeks. Once the data is collected the building operator or engineer can open the Excel tool, upload and process the data. Once the program is finished running the customer will see an output similar to Figure 44. The tool automatically calculates the rate of change of power vs. flow and recommends an upper and lower delta-T and flow setpoint based on either a comfort or energy savings priority. With this visual aid the user will be able to clearly identify the saturation point of the coil between the upper and lower threshold values identified in Figure 44. Setting a delta-T or flow limit at the upper threshold (red dot in Figure 44) will lead to power savings by limiting the flow at 45 gpm. Past this point, an increase in flow rate does not significantly increase the cooling power of the coil enough to warrant the extra pumping power required. However, it may also be necessary to maximize energy savings potential by limiting the flow before this point. By recommending a lower threshold setpoint of 36 gpm (yellow dot in Figure 44) the customer will have the opportunity to decrease the flow required even further, thus saving on pump energy. The Excel tool calculates upper and lower setpoints for both delta-T and flow limit. The user can then choose whether to use the upper setpoint based on a comfort priority or the lower setpoint based on an energy savings priority.

It should also be mentioned that the reason for providing two setpoints is motivated from the fact that for some systems it would be beneficial to limit the flow earlier in order to maximize energy savings potential. There will be cases that this is not desirable which is why a more conservative setpoint based on the higher threshold is recommended. The Excel tool is currently being tested on a control valve in a building at Busch Gardens Florida.

## 7.4 – Power Limiting Strategy

Ideally, it would be nice to leave the customer out of the equation. Due to the slight error in the setpoint calculations and potential error of the customer when using the Excel tool, it would be beneficial to design logic for the actuator that adaptively finds the proper flow limit continuously, thus eliminating the need for outside data acquisition and calculation. The valve could then adapt and adjust itself to the particular coil it is controlling. An approach was investigated in which the

maximum power of the coil is calculated using a simple sorting algorithm and a set of conditional statements. It should be noted that the power limiting strategy is quite simple and needs to be further researched but it illustrates the direction that the technology is headed.

If the maximum operating capacity of a coil can be internally calculated, the saturation point of the coil could be defined as a percentage of the maximum power of that particular coil. For example, when looking at Figure 31 it appears that the maximum power is approximately 100, kW at a flow rate of 4.2 kg/s. A limit set at 90% of the max power would be equivalent to limiting the flow at 2.6 kg/s. Setting a flow limit would also be less sensitive to SWT fluctuations. To take it even one step further a max power could be estimated for each SWT set. The limiting point of the coil could then be adjusted according to the SWT thus eliminating the effect that SWT fluctuations have on the heat transfer within the coil. This could potentially save large amounts of energy.

The algorithm developed analyzes data collected for one month. The algorithm attempts to find the maximum power while disregarding outliers and any other disturbances in the system and has the following structure:

1. Gather data in vector form (time series) for a period of at least 2 weeks.
    - Column 1 – mass flow rate
    - Column 2 – cooling power
2. Sort data into bins by increasing mass flow rate

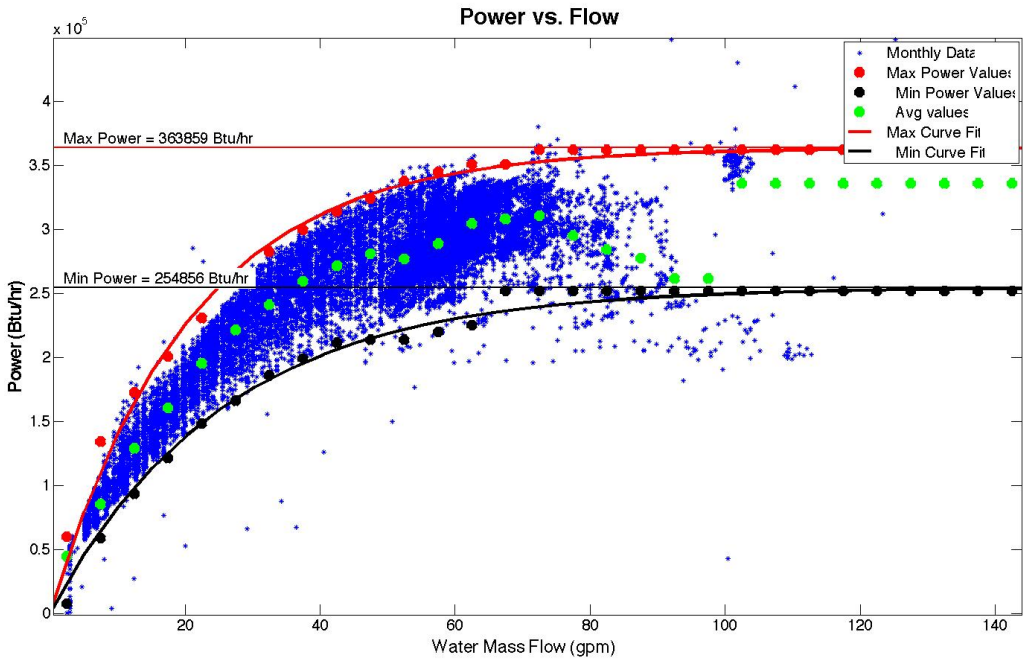


**Figure 45 - Algorithm results using July data**

3. Define a mass flow interval size to categorize data and give it a set number. For instance set 1 will contain power values at 0 - 5 l/s water mass flow, set 2 - power values at 5 - 10 l/s water mass flow, set 3 - power values at 10 - 15 l/s, etc.
4. Step through each set starting with set 1
5. Calculate characteristics of each set and compare with the previous set. For example, density of data, minimum power, max power and average power are all recorded as the current set and then compared to a previous set.
6. Converge on a max and min power value and output results

Let us examine Figure 45 a bit closer by drawing our attention to the red, black and green data points. The data in Figure 45 is analyzed set-by-set starting with values between 0 and 5 gpm. Maximum, minimum, average power and number of points are calculated for the current set then compared with the previous set. If the rate of change of values from the previous set to the current set is negative then the value from the previous set is passed on. If the rate of change is positive then the value is accepted and the next set is analyzed. The algorithm also considers the density of points when determining to release or hold a value. When considering Figure 45 the density of point's decreases drastically at 75 gpm. When the density of points is below a minimum threshold the previous value is accepted. This can be seen as the point when the calculated max/min power remains constant. This prevents the algorithm from estimating a decreasing power value. Finally the maximum and minimum capacity of the coil is estimated.

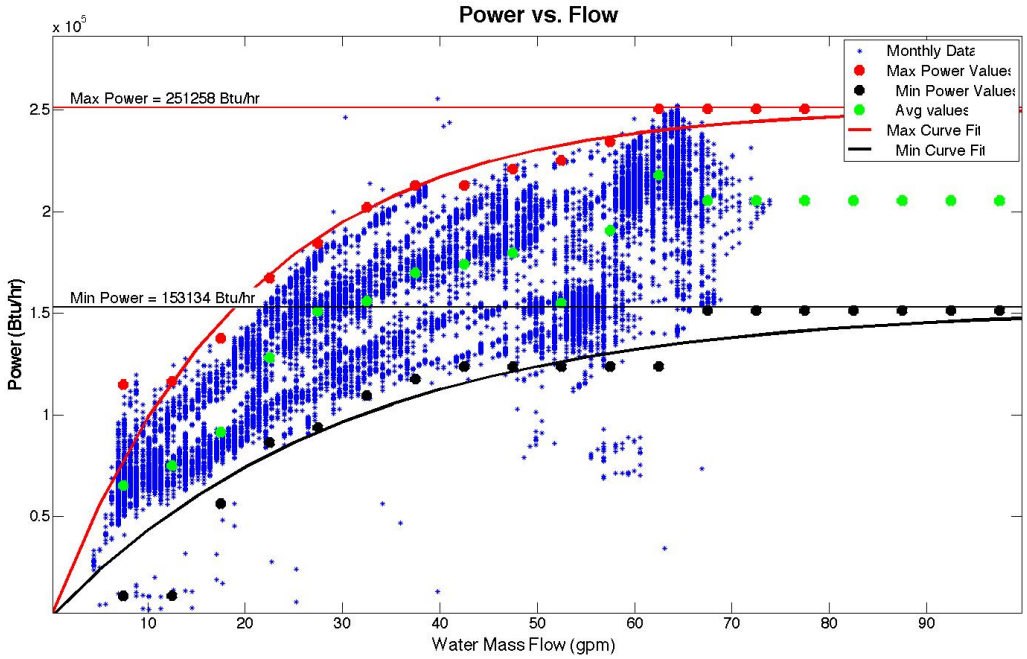


**Figure 46 – Max/min power calculation for AHU-2**

This simple algorithm was tested using data from two other AHU's at MIT and proved to converge on a max/min power value quite easily as seen in Figure 46 and Figure 47.

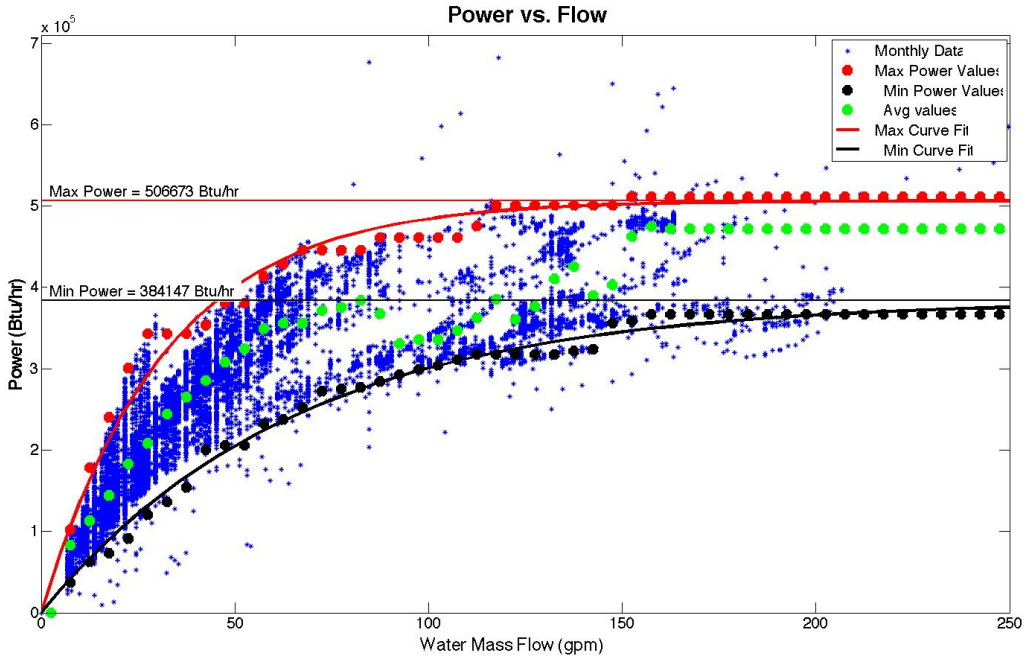


**Figure 47 – Max/min power calculation for AHU-1**

The method for finding the max/min power output of a coil needs to be investigated further to realize the full scope of energy saving potential, although it is evident that the potential is there at the pump level. By having a better understanding of how a coil behaves in an actual system it will enable intelligent control devices to better control the water flow through the coil, thus saving pump energy. Energy savings could also be realized in the central plant by optimizing the return temperature of the chilled water with the use of intelligent actuators. Chiller efficiency is affected when the return water temperature is too low. As mentioned in the literature review this can have a negative effect on chiller performance, which is a source of wasted energy in the central plant. A higher delta-T will have a positive effect on the central plant. The combined energy savings potential at both the pump and plant level in a large building is significant and should be considered when designing such systems.

# References


Applied Flow Technology Corp. "Applied Flow Technology." *Customer Profiles*. March 20, 2007. http://www.aft.com/dmdocuments/tme_profile.pdf (accessed December 5, 2011).

Arnold, Scott. "Pressure Independent Valves Simplify Air Base's Transition to Variable Flow." *HPAC Engineering*, November 2007: 38-39.

Brandemuehl, M. J., S. Gabel, and I. Andersen. *Toolkit for HVAV System Energy Calculations*. Fortran Code, University of Colorado at Boulder, Boulder: ASHRAE, 1993.

Braun, J. E., S. A. Klein, and J. W. Mitchell. "Effectiveness Models for Cooling Towers and Cooling Coils." *ASHRAE Transactions* 95, no. 2 (1989): 164-174.

Dilliot, John. "2008 Best Practice Case Studies." *Green Building Research Center UC Berkeley*. January 5, 2008. http://greenbuildings.berkeley.edu/pdfs/bp2008_ucsd_retrofit.pdf (accessed September 22, 2011).

Elmahdy, A. H., and G. P. Mitalas. "A Simple Model for Cooling and Dehumidifying Coils for Use in Calculating Energy Requirements for Buildings." *ASHRAE Transactions* 83 (1977): 102-118.

Elmahdy, Dr. A. H., and R. C. Biggs. "Efficiency of Extended Surface with Simulatneous Heat and Mass Transfer." *ASHRAE Transactions* 89 (1983): 135-143.

Elmahdy, DR. A. H. "Finned Tube Heat Exchanger: Correlation fo Dry Surface Heat Transfer Data." *ASHRAE Transactions* Part 2 (1979): 262-273.

Fiorino, Donald P. "Achieving High Chilled-Water Delta T's." *ASHRAE Journal*, November 1999: 24-30.

Henze, Gregor P, and Alexander G Floss. "Evaluation of temperature degradation in hydraulic flow networks." *Energy and Buildings*, 2011: 1820 - 1828.

Hyman, Lucas B., and Don Little. "Overcoming Low Delta-T, Negative Delta-P at Large University Campus." *ASHRAE Journal*, February 2004: 28-34.

Lemort, Vincent, and Jean Lebrun. "Developement of Simple Cooling Coil Models for Simulation of HVAC Systems." *ASHRAE Transactions*, 2008: 319-328.

McQuiston, Faye, Jerald Parker, and Jeffrey Spitler. *Heating, Ventilating, and Air Conditioning*. Edited by Sixth. Danvers: John Whley & Sons, Inc., 2005.

Taylor, Steven T. "Degrading Chilled Water Plant Delta-T; Causes and Mitigation." *ASHRAE Transactions* 108 (2002): 1-13.

Wang, Gang, Mingsheng Liu, and David E. Claridge. "Decoupled Modeling of Chilled-Water Cooling Coils." *ASHRAE Transactions*, 2007: 484-493.

Wetter, Michael. *Simulation Model Finned Water-to-Air Coil without Condensation.* Simulation Model, Lawrence Berkeley National Laboratory, 1998.

Xiatang, Zhou, and James E. Braun. *A Simplified Dynamic Model for Chilled-Water Cooling and Dehumidifying Coils - Part 1: Developement.* Vol. 13, in *HVAC&R Research*, by ASHRAE, 785-803. London: Taylor & Francis Group, 2007.

Zhou, Xiaotang, and James E. Braun. "An Inverse Model for Transient Cooling and Dehumidifying Coil Performance." *ASHRAE Transactions*, 2008: 308-318.

Zhou, Xiaotang, James E. Braun, and Qingfan Zeng. *An Improved Method for Determining Heat Transfer Fin Efficiencies for Dehumidifying Cooling Coils.* Vol. 13, in *HVAC&R Research*, by ASHRAE, 769-783. London: Taylor & Francis Group, 2007.